PRG 018 ©October 2015

QUEEN'S UNIVERSITY

POLYMERS RESEARCH GROUP

19 Division Street, Kingston, ON, K7L 3N6 Canada

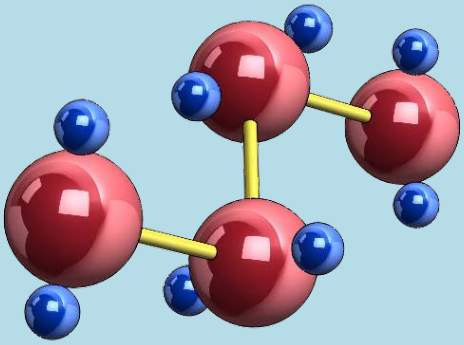

POLYMER FLUID DYNAMICS: CONTINUUM AND MOLECULAR APPROACHES

R.B. Bird[1] and A.J. Giacomin[2,*]

[1]Rheology Research Center and Chemical and Biological Engineering Department
University of Wisconsin-Madison, Madison, WI 53706

[2]Chemical Engineering Department and Polymers Research Group
Mechanical and Materials Engineering Department
Queen's University, Kingston, ON K7L 3N6

*Corresponding author (giacomin@queensu.ca)

QU-CHEE-PRG-TR--2015-18

POLYMER FLUID DYNAMICS: CONTINUUM AND MOLECULAR APPROACHES

R.B. Bird[1] and A.J. Giacomin[2,*]

[1]Rheology Research Center
Chemical and Biological Engineering Department
University of Wisconsin-Madison
Madison, WI 53706

[2]Chemical Engineering Department, Polymers Research Group
Mechanical and Materials Engineering Department
Queen's University
Kingston, ON K7L 3N6

ABSTRACT

To solve problems in polymer fluid dynamics, one needs the equation of continuity, motion, and energy. The last two equations contain the stress tensor and the heat-flux vector for the material. There are two ways to formulate the stress tensor: (1) one can write a continuum expression for the stress tensor in terms of kinematic tensors, or (2) one can select a molecular model that represents the polymer molecule, and then develop an expression for the stress tensor from kinetic theory. The advantage of the kinetic theory approach is that one gets information about the relation between the molecular structure of the polymers and the rheological properties.

In this review, we restrict the discussion primarily to the simplest stress tensor expressions or "constitutive equations" containing from two to four adjustable parameters, although we do indicate how these formulations may be extended to give more complicated expressions. We also explore how these simplest expressions are recovered as special cases of a more general framework, the Oldroyd 8-constant model. The virtue of studying the simplest models is that we can discover some general notions as to which types of empiricisms or which types of molecular models seem to be worth investigating further. We also explore equivalences between continuum and molecular approaches.

We restrict the discussion to several types of simple flows, such as shearing flows and extensional flows. These are the flows that are of greatest importance in industrial operations. Furthermore, if these simple flows cannot be well described by continuum or molecular models, then it is not necessary to lavish time and energy to apply them to more complex flow problems.

*Corresponding author (giacomin@queensu.ca)

CONTENTS

FIGURES

TABLES

I. SIMPLE FLOW FIELDS

The stress responses to flow are governed by the equation of motion, here written in compact form, in terms of the (extra) stress tensor $\boldsymbol{\tau}$:

$$\frac{\partial}{\partial t}\rho\mathbf{v} = -\left[\nabla\cdot\left(\rho\mathbf{v}\mathbf{v} + p\boldsymbol{\delta} + \boldsymbol{\tau}\right)\right] + \rho\mathbf{g} \tag{1}$$

In this summary, we consider the stress responses to two classes of flows (§8.2 of [1]), *shear flows* and *extensional flows*. We define these flows below, in Eqs. (2) and (3), as solutions to Eq. (1), subject to (i) appropriate velocity boundary conditions, and (ii) neglect of fluid inertia and gravity.

a. Shear Flows

Shear flows are defined by

$$\begin{bmatrix} v_x\left(y,t\right) = \dot{\gamma}^0\left(t\right)y \\ v_y = v_z = 0 \end{bmatrix} \text{ with } \begin{bmatrix} \dot{\gamma}^0\left(t\right) = \dot{\gamma}^0, \text{a constant} & \text{(a)} \\ \dot{\gamma}^0\left(t\right) = \dot{\gamma}^0\cos\omega t, \text{with } \dot{\gamma}^0 \text{ very small} & \text{(b)} \\ \dot{\gamma}^0\left(t\right) = \dot{\gamma}^0\cos\omega t, \text{with } \dot{\gamma}^0 \text{ large} & \text{(c)} \end{bmatrix} \tag{2}$$

where v_x, v_y, and v_z are the velocity components, and $\dot{\gamma}^0$ is the shear rate. Since the velocity in the flow direction, v_x, is taken to be

proportional to y, the flow is homogeneous. The three cases considered here are (a) steady shear flow, (b) small-amplitude oscillatory shear (SAOS) flow, and (c) large-amplitude oscillatory shear (LAOS) flow. Other time dependent flows (such as stress relaxation) could also be discussed (Figure 4.3-1 of [11]).

b. Extensional Flows

Extensional flows are defined by

$$\begin{bmatrix} v_z(z,t) = \dot{\varepsilon}^0(t) z \\ v_x = v_y = -\frac{1}{2} v_z \end{bmatrix} \text{ with } \dot{\varepsilon}^0(t) = \dot{\varepsilon}^0, \text{ a constant} \tag{3}$$

Here we restrict ourselves to steady extensional flow. A variety of time dependent extensional flows can be studied, including oscillatory flows and stress relaxation. If $\dot{\varepsilon}^0(t)$ is taken to be negative, the flow is called biaxial extension.

II. SIMPLE CONTINUUM MODELS

The simplest continuum models for polymeric liquids are those that contain just two parameters. By *continuum* models, we mean models that ignore the molecules or molecular chains from which the

polymeric liquids are composed. Instead, continuum models are sophisticated guesses based on some knowledge of the measured behavior of the polymeric liquids. We consider two Maxwell models, some of their modifications, and a more general framework that contains all of these modifications as special cases.

a. Convected Maxwell

This contravariant convected model is a nonlinear version of the linear model $\boldsymbol{\tau} + \lambda\left(\partial\boldsymbol{\tau}/\partial t\right) = -\eta_0\dot{\boldsymbol{\gamma}}$ originally proposed by Maxwell ([2]; see §8.4 of [1])

$$\boldsymbol{\tau} + \lambda\boldsymbol{\tau}_{(1)} = -\eta_0\dot{\boldsymbol{\gamma}} \tag{4}$$

in which $\boldsymbol{\tau}$ is the (extra) stress tensor, and its convected derivative is: $\boldsymbol{\tau}_{(1)} = D\boldsymbol{\tau}/Dt - \left\{\boldsymbol{\tau}\cdot\nabla\mathbf{v}\right\}^{\dagger} - \left\{\boldsymbol{\tau}\cdot\nabla\mathbf{v}\right\}$ for a symmetric $\boldsymbol{\tau}$, D/Dt is the substantial derivative, $\dagger$ indicates the transpose of a tensor, and $\dot{\boldsymbol{\gamma}} = \left(\nabla\mathbf{v}\right)^{\dagger} + \nabla\mathbf{v}$ is the rate of deformation tensor (see Eq. 8.3-2 of [1]). The two constants are λ, the time constant, and η_0, the zero-shear-rate viscosity. This model (see §7.2 of [3]) can also be regarded as a truncated version of the Oldroyd 8-constant model [4] (see § II.c).

Next we give two important modifications of the contravariant convected Maxwell model:

i. Jeffreys

By adding one additional time constant, we get

$$\boldsymbol{\tau} + \lambda_1 \boldsymbol{\tau}_{(1)} = -\eta_0 \left(\dot{\boldsymbol{\gamma}} + \lambda_2 \dot{\boldsymbol{\gamma}}_{(1)} \right) \tag{5}$$

where λ_1 and λ_2 are time constants, and where $\eta_\infty / \eta_0 = \lambda_2 / \lambda_1$, η_∞ being the infinite-shear-rate viscosity. This model is sometimes called the "Oldroyd-B model". Jeffreys originally cast Eq. (5) with ordinary derivatives (see Problem 14·422 of [5] or Problem 14·422 of [6]).

ii. Generalized Convected Maxwell

By superposing an infinitude of Maxwell models, there results

$$\boldsymbol{\tau} = \sum_{k=1}^{\infty} \boldsymbol{\tau}_k \quad \text{where} \quad \boldsymbol{\tau}_k + \lambda_k \boldsymbol{\tau}_{k(1)} = -\eta_k \dot{\boldsymbol{\gamma}} \tag{6}$$

in which λ_k and η_k are, respectively, infinite sets of constants with dimensions of time and viscosity. When the Spriggs relations [7,8] are used:

$$\lambda_k = \lambda / k^{\alpha} \text{ and } \eta_k = \eta_0 \lambda_k / \Sigma_k \lambda_k , \tag{7}$$

the number of constants is reduced from infinity to three: the zero-shear-rate viscosity η_0, one time constant λ, and a dimensionless constant α.

b. Corotational Maxwell

This model is another type of nonlinear extension of the original Maxwell model ([9,10,17,18]; Chapter 7 of [11]; §8.5 of [1])

$$\boldsymbol{\tau} + \lambda \left(\mathscr{D} \boldsymbol{\tau} / \mathscr{D} t \right) = -\eta_0 \dot{\boldsymbol{\gamma}} \tag{8}$$

in which $\mathscr{D} \boldsymbol{\tau} / \mathscr{D} t = \left(D\boldsymbol{\tau} / Dt \right) + \frac{1}{2} \left\{ \boldsymbol{\omega} \cdot \boldsymbol{\tau} + \boldsymbol{\tau} \cdot \boldsymbol{\omega} \right\}$ is the *corotational* (or *Jaumann*) *derivative* [12, 13], and $\boldsymbol{\omega} = \nabla \mathbf{v} - \left(\nabla \mathbf{v} \right)^{\dagger}$ is the *vorticity tensor*. This model is sometimes called the Zaremba-Fromm-Dewitt (ZFD) model [9,14,15]. The corotational Maxwell model may be viewed as a truncated form of the Oldroyd 8-constant model [16] (see § II.c). Important modifications of this model are:

i. Jeffreys

This is a three-constant model [17, 18], analogous to the codeformational Jeffreys model (Eq. (5) above)

$$\boldsymbol{\tau} + \lambda_1 \left(\mathscr{D} \boldsymbol{\tau} / \mathscr{D} t \right) = -\eta_0 \left(\dot{\boldsymbol{\gamma}} + \lambda_2 \mathscr{D} \dot{\boldsymbol{\gamma}} / \mathscr{D} t \right) \tag{9}$$

containing two time constants, λ_1 and λ_2, and where $\eta_\infty / \eta_0 = \lambda_2 / \lambda_1$, where $\eta_\infty = \lim_{\dot{\gamma} \to \infty} \eta(\dot{\gamma})$.

ii. Arbitrary Normal Stress Ratio (ANSR)

This three-constant model is [10]:

$$\boldsymbol{\tau} + \lambda_1 \left(\mathscr{D} \boldsymbol{\tau} / \mathscr{D} t \right) = -\eta_0 \dot{\boldsymbol{\gamma}} + \lambda_0 \left\{ \boldsymbol{\tau} \cdot \dot{\boldsymbol{\gamma}} + \dot{\boldsymbol{\gamma}} \cdot \boldsymbol{\tau} \right\} \tag{10}$$

contains two time constants λ and λ_0 where minus the normal stress coefficient ratio is given by $-\Psi_2 / \Psi_1 = -\left(\tau_{yy} - \tau_{zz} \right) / \left(\tau_{xx} - \tau_{yy} \right) = \frac{1}{2} \left[1 - \left(\lambda_0 / \lambda \right) \right]$ (see § V.b below).

iii. Generalized Corotational Maxwell

This is the analog of the superposition of codeformational Maxwell models:

$$\boldsymbol{\tau} = \sum_{k=1}^{\infty} \boldsymbol{\tau}_k \text{ where } \boldsymbol{\tau}_k + \lambda_k \frac{\mathscr{D}\boldsymbol{\tau}_k}{\mathscr{D}t} = -\eta_k \dot{\boldsymbol{\gamma}} \tag{11}$$

The Spriggs relations (see § II.a.ii above) may be used to reduce the number of constants from infinity to three.

c. Oldroyd 8-constant

To create a continuum model with more flexibility than the simple two and three constant models, Oldroyd suggested [4,16]

$$\begin{aligned} &\boldsymbol{\tau} + \lambda_1 \frac{\mathscr{D}\boldsymbol{\tau}}{\mathscr{D}t} + \tfrac{1}{2}\mu_0 \left(\operatorname{tr}\boldsymbol{\tau}\right)\dot{\boldsymbol{\gamma}} - \tfrac{1}{2}\mu_1 \left\{\boldsymbol{\tau}\cdot\dot{\boldsymbol{\gamma}} + \dot{\boldsymbol{\gamma}}\cdot\boldsymbol{\tau}\right\} + \tfrac{1}{2}\nu_1 \left(\boldsymbol{\tau}:\dot{\boldsymbol{\gamma}}\right)\boldsymbol{\delta} \\ &\quad = -\eta_0 \left[\dot{\boldsymbol{\gamma}} + \lambda_2 \frac{\mathscr{D}\dot{\boldsymbol{\gamma}}}{\mathscr{D}t} - \mu_2 \left\{\dot{\boldsymbol{\gamma}}\cdot\dot{\boldsymbol{\gamma}}\right\} + \tfrac{1}{2}\nu_2 \left(\dot{\boldsymbol{\gamma}}:\dot{\boldsymbol{\gamma}}\right)\boldsymbol{\delta}\right] \end{aligned} \tag{12}$$

On the left side he included all possible products of the $\boldsymbol{\tau}$ and $\dot{\boldsymbol{\gamma}}$ tensors, and on the right side, all possible terms quadratic in $\dot{\boldsymbol{\gamma}}$. Eq. (12) contains the corotational Maxwell and Jeffreys models, as well as the ANSR model, the codeformational Maxwell model, the 3-constant Oldroyd model used by Williams [19], and the second-order fluid [see after Eq. (13)]. Usually both terms in Eq. (12) containing the double-dot product are omitted, inasmuch as they contribute only an undetermined isotropic term. This is then called the "Oldroyd-6 model."

d. Retarded Motion Expansion

Popular among applied mathematicians has been the retarded motion expansion, an expansion of the stress tensor in terms of the rate-of-strain tensor and its Jaumann derivatives

$$\begin{aligned}\boldsymbol{\tau} = &-\alpha_1\dot{\boldsymbol{\gamma}} + \alpha_2\frac{\mathscr{D}}{\mathscr{D}t}\dot{\boldsymbol{\gamma}} - \alpha_{11}\left\{\dot{\boldsymbol{\gamma}}\cdot\dot{\boldsymbol{\gamma}}\right\} \\ &-\alpha_3\frac{\mathscr{D}^2}{\mathscr{D}t^2}\dot{\boldsymbol{\gamma}} + \alpha_{12}\left\{\dot{\boldsymbol{\gamma}}\cdot\left(\frac{\mathscr{D}}{\mathscr{D}t}\dot{\boldsymbol{\gamma}}\right) + \left(\frac{\mathscr{D}}{\mathscr{D}t}\dot{\boldsymbol{\gamma}}\right)\cdot\dot{\boldsymbol{\gamma}}\right\} - \alpha_{1:11}\left(\dot{\boldsymbol{\gamma}}:\dot{\boldsymbol{\gamma}}\right)\dot{\boldsymbol{\gamma}} - \cdots\end{aligned} \tag{13}$$

in which the α's are constants. If only one term is included on the right side, this gives the Newtonian fluid; if three terms are included, the result is called the *second-order fluid*; and with six terms, the *third-order fluid*, and so on. As a constitutive equation it is limited to slow flows that are slowly varying in time. Any of the continuum equations may be expanded in the form of a retarded motion equation and the relations between them found. For example, for the Oldroyd-6 model, the interrelations of the parameters are (see p. 406 of [11]):

$$\begin{aligned}&\alpha_1 = \eta_0 \qquad \alpha_2 = \eta_0\left(\lambda_1 - \lambda_2\right) \qquad \alpha_3 = \eta_0\lambda_1\left(\lambda_1 - \lambda_2\right) \qquad \alpha_{11} = \eta_0\left(\mu_1 - \mu_2\right) \\ &\alpha_{12} = \eta_0\left[\lambda_1\left(\mu_1 - \mu_2\right) + \tfrac{1}{2}\mu_1\left(\lambda_1 - \lambda_2\right)\right] \qquad \alpha_{1:11} = \tfrac{1}{2}\eta_0\left(\mu_1 - \mu_0\right)\left(\mu_1 - \mu_2\right)\end{aligned} \tag{14}$$

III. SIMPLE MOLECULAR MODELS

Here we restrict ourselves, for the most part, to molecular models of polymeric liquids containing only two parameters plus a Newtonian solvent viscosity, η_s, and modifications thereof. We examine these models for their ability to predict, at least qualitatively, observed viscoelastic behaviors [20].

For rigid molecular models such as rigid dumbbells, we describe the probability of an orientation (θ,ϕ) by an *orientational distribution*, $\psi(\theta,\phi)$. For elastic models such as elastic dumbbells, we describe the configuration with a *configurational distribution*, $\Psi(R,\theta,\phi)$, where R is the dumbbell length. Whereas $\psi(\theta,\phi)$ just contains orientation information, $\Psi(R,\theta,\phi)$ also contains information about the extension of the molecule. The advantage of molecular models over continuum models is that they connect $\psi(\theta,\phi)$ or $\Psi(R,\theta,\phi)$ to the stresses in the fluid and thus, to rheology. For time-dependent flows, such as oscillatory shear flow, molecular models can connect the evolving molecular orientations or configurations, $\psi(\theta,\phi,t)$ or $\Psi(R,\theta,\phi,t)$, to the fluid rheology.

To connect $\Psi(R,\theta,\phi,t)$ to evolving stresses we average over

configuration space:

$$\left\langle F\left(R,\theta,\phi,t\right)\right\rangle = \int_0^{2\pi}\int_0^{\pi}\int_0^{\infty} F\left(R,\theta,\phi,t\right)R^2\,dR\sin\theta\,d\theta\,d\phi \tag{15}$$

and to connect $\psi(\theta,\phi,t)$ to evolving stresses, we average over orientation space:

$$\left\langle f\left(\theta,\phi,t\right)\right\rangle = \int_0^{2\pi}\int_0^{\pi} f\left(\theta,\phi,t\right)\sin\theta\,d\theta\,d\phi \tag{16}$$

which is just Eq. (15) evaluated for constant R. Whereas $\psi(\theta,\phi,t)$ is dimensionless, $\Psi(R,\theta,\phi,t)$ has dimensions of volume. Since ψ and Ψ have different dimensions and since they depend on different variables, the same symbol ψ is often used for both $\psi(\theta,\phi,t)$ and $\Psi(R,\theta,\phi,t)$, without loss of clarity [8,29].

a. Elastic Dumbbell

In this subsection we discuss elastic dumbbells, beginning with linear (Hookean) spring connectors, followed by several nonlinear types of springs.

i. Hookean

The macromolecule is modeled as a pair of identical beads of

radius r_0 connected by a massless, dimensionless spring with a spring constant H (see Figure **1**). That is, the force between the beads is given by $\mathbf{F}^{(c)} = H\mathbf{R}$, $\mathbf{F}^{(c)}$ being the force vector in the connecting spring (where the $^{(c)}$ indicates the connector), and $\mathbf{R}$ the vector between the bead centers (so that the dumbbell length R is simply the magnitude of $\mathbf{R}$). These Hookean dumbbells are suspended in a Newtonian solvent (see §13.4 of [8]) . Then, it can be assumed that the stress tensor is given by $\boldsymbol{\tau} = \boldsymbol{\tau}_s + \boldsymbol{\tau}_p$, the solvent contribution being $\boldsymbol{\tau}_s = -\eta_s \dot{\boldsymbol{\gamma}}$ and the polymer contribution that is described by

$$\boldsymbol{\tau}_p + \lambda_H \boldsymbol{\tau}_{p(1)} = -nkT\lambda_{\mathrm{H}} \dot{\boldsymbol{\gamma}} \tag{17}$$

which has the form of Eq. (4), the convected Maxwell model. The time constant λ_H is given by $\zeta / 4H$, in which $\zeta = 6\pi\eta_s r_0$, this being the Stokes law drag coefficient for a sphere of radius r_0 moving through the solvent. We identify $nkT\lambda_{\mathrm{H}}$ with the dumbbell contribution to the zero-shear-rate viscosity, $\eta_0 - \eta_s$. This kind of dumbbell allows for infinite stretching of the molecule, which is unrealistic. When suspended in a fluid at rest, these dumbbells have an average length $H\left\langle R^2 \right\rangle / kT$. The zero-shear-rate viscosity is given by $\eta_0 = \eta_s + nkT\lambda_H$, a constant.

Now let us examine modifications of the elastic dumbbell:

ii. Finitely Extensible Nonlinear Elastic (FENE-P)

To permit the molecule to stretch only up to a certain length L, we can replace the expression above for $\mathbf{F}^{(c)}$ by (Example 13.5-2 of [8]),

$$\mathbf{F}^{(c)} = H\mathbf{R}\Big/\Big(1-\big(R^2/L^2\big)\Big) \cong H\mathbf{R}\Big/\Big(1-\big\langle R^2/L^2\big\rangle\Big) \tag{18}$$

We thus call this molecular model finitely extensible, and the replacement of $\big(R^2/L^2\big)$ by $\big\langle R^2/L^2\big\rangle$, the Peterlin approximation [21]. Eq. (18) leads to the following approximate expression for the polymer contribution to the stress tensor (Eq. (8.6-4) of [1]; Eq. (13.5-56) of [8] with $\varepsilon = 0$; [22]):

$$Z\boldsymbol{\tau}_p + \lambda_H\boldsymbol{\tau}_{p(1)} - \lambda_H\Big[\boldsymbol{\tau}_p - nkT\boldsymbol{\delta}\Big]\big(D\ln Z/Dt\big) = -nkT\lambda_{\mathrm{H}}\dot{\boldsymbol{\gamma}} \tag{19}$$

Here $Z = 1+\big(3/b\big)\Big[1-\big(\mathrm{tr}\,\boldsymbol{\tau}_p/3nkT\big)\Big]$ in which $b = HL^2/kT$.

iii. Fraenkel

This dumbbell has a straight connector that oscillates at very small amplitude about a length L (even for a liquid at rest), so that the

force is given by ([23,24,25]; §10.3 of [8]; Table 11.5-1 of [8])

$$\mathbf{F}^{(c)} = H\left(1-\frac{L}{R}\right)\mathbf{R} \tag{20}$$

where L is the dumbbell length when $\mathbf{F}^{(c)}$ is zero. When $L \to 0$, the model reduces to the Hookean dumbbell; and when $H \to \infty$, we get a rigid dumbbell of length L (see Figure **1**). The latter limit leads to the following approximate expression for the polymer contribution to the stress tensor for a *Fraenkel dumbbell*

$$Z\boldsymbol{\tau}_p + \lambda_H \boldsymbol{\tau}_{p(1)} - \lambda_H\left(\boldsymbol{\tau}_p - nkT\boldsymbol{\delta}\right)\left(D\ \ln Z/Dt\right) = -nkT\lambda_H\dot{\boldsymbol{\gamma}} \tag{21}$$

where $\lambda_H = \zeta/4H$, $b = HL^2/kT$, $Z\left(\text{tr}\,\boldsymbol{\tau}_p\right) = \left(1-\mathscr{T}\right)/\left(1-\mathscr{T}+\frac{1}{3}b\right)$, and $\mathscr{T} = \left(\text{tr}\,\boldsymbol{\tau}_p\right)/3nkT$ (see Problem 13B.11 of [8]).

b. Rigid Dumbbell

In this subsection we concern ourselves with rigid models, starting with two-bead dumbbells, and then turning to multi-bead rods.

i. Two-Bead Rod

The rigid dumbbell consists of two spherical beads of radius r_0

connected by a rigid, massless, dimensionless rod such that the bead centers are separated by a distance L (see Figure **1**). This rigid dumbbell is suspended in a Newtonian liquid of viscosity, η_s. We use the stress tensor expression given by Giesekus (26; Table 14.3-1 of [8])

$$\boldsymbol{\tau}_p = -\eta_s \dot{\boldsymbol{\gamma}} + 3nkT\lambda \left\langle \mathbf{uu} \right\rangle_{(1)} \tag{22}$$

in which $\mathbf{u}$ is the unit vector pointing along the rod, and $\lambda = \zeta L^2 / 12kT$ is the time constant for the polymer, with ζ being the drag coefficient for a single bead (see Table 14.3-1 of [8]). Here, we identify $nkT\lambda$ with the dumbbell contribution to the zero-shear-rate viscosity, $\eta_0 - \eta_s$. To evaluate the quantity inside the $\langle\ \rangle$, which is an average over all orientations, it is therefore necessary, to find the orientational distribution function for the rigid dumbbells ([27, 28]; Chapter 11 of [29]; Chapter 13 of [8]).

ii. Multi-bead Rod

We next consider the model designed for rigid, rodlike molecules (§14.3 of [8]). This molecular model consists of a rod of length L with N spheres of radius r_0 distributed uniformly along the rod. Then all the results for the 2-bead model (dumbbell) can be taken over at once

by replacing λ by $\lambda_N = \zeta L^2 N(N+1)/72(N-1)kT$. Thus here, we identify $nkT\lambda_N$ with the multi-bead rod contribution to the zero-shear-rate viscosity, $\eta_0 - \eta_s$. Therefore the behaviors of the two systems are qualitatively alike.

For both the rigid dumbbell and the multi-bead dumbbell, hydrodynamic interaction may matter. By *hydrodynamic interaction* we mean the disturbances of the flow field near one bead because of the motion of neighboring beads. These disturbances matter when the beads are close to one another, but these disturbances just modify the relaxation time, leaving the behaviors of the models closely resembling their interactionless counterparts (§14.6 of [8]).

iii. Mixture of Rigid Dumbbells

A polydisperse system may be approximated by a mixture of dumbbells, with the mole fraction of dumbbells of length L_j being x_j , all suspended in a solvent of viscosity η_s. For this system, there will be a set of time constants $\lambda_j = \zeta L_j^2/12kT$, where ζ is the drag coefficient for a single bead (see §11.3 of [8]). The Spriggs relations

(see § II.a.ii above) may be used to reduce the number of constants from infinity to three.

c. Chain

Thus far, all of our molecular models have been straight. In this subsection, we turn our attention to flexible chains. Whereas each straight molecular model gives a single relaxation time (see § III.a and § III.b above), each chain model gives a discrete spectrum of relaxation times, the number of times increasing with number of chain links. For chains, we identify $nkT\sum_j \lambda_j$ with the chain contribution to the zero-shear-rate viscosity, $\eta_0 - \eta_s$.

i. Rouse and Zimm Freely Jointed

If *N* beads are joined by Hookean springs, end to end, in a freely jointed chain, we get the Rouse chain [30], used extensively by polymer chemists for several decades (see Figure **2**). Then it can be shown that the stress tensor is given by $\boldsymbol{\tau} = \boldsymbol{\tau}_s + \boldsymbol{\tau}_p$, the solvent contribution being $\boldsymbol{\tau}_s = -\eta_s \dot{\boldsymbol{\gamma}}$ and the polymer contribution being

$\boldsymbol{\tau}_p = \sum_j \boldsymbol{\tau}_j$ where

$$\boldsymbol{\tau}_j + \lambda_j \boldsymbol{\tau}_{j(1)} = -nkT\lambda_j \dot{\boldsymbol{\gamma}} \tag{23}$$

where the discrete relaxation spectrum is given by:

$$\lambda_j = \frac{\lambda_R}{\sin^2\left(j\pi/2N\right)};\ \eta_j = nkT\lambda_j \tag{24}$$

where the *longest relaxation time* is given by $\lambda_R = \zeta/\left(8H\right)$ (§15.3 of [8]. For the longest chains, in the limit of large N, we recover the first of the Spriggs relations in Eq. (7) with $\alpha = 2$, but not the second. This chain model may be further modified by including the hydrodynamic interactions between beads, be they adjacent or not; it is then called the Zimm model ([31]; §15.4 of [8]). Strictly, the Rouse and Zimm chains are generalizations of the original *linear* model of Maxwell, that is, by replacing $\boldsymbol{\tau}_{j(1)}$ in Eq. (6) by $\partial\boldsymbol{\tau}_j/\partial t$.

ii. Kramers Freely Jointed

One can connect N beads by rigid rods in a freely jointed chain (see Figure **2**) to depict a flexible macromolecule ([32,33], see §11.3, §16.1 and §16.4 §16.6 of [8]). The Curtiss-Bird theory, designed for

polymer melts, makes use of the Kramers chain model (see Chapter 19 of [8]; [34,35,36,37,38,39,40,41,58]).

iii. Mixtures of Chains

A polydisperse system may be approximated by a mixture of chains, all suspended in a solvent of viscosity η_s. There will then be an infinite set of longest relaxations times, one for each chain, λ_{Rj}. The Spriggs relations (see § II.a.ii above) may then be used to reduce the number of constants from infinity to three.

IV. CONTINUUM-MOLECULAR CONNECTIONS

As we shall see in subsequent sections, predicted behaviors for molecular and continuum models, in both small-amplitude oscillatory shear flow, and in steady shear flow, are both reasonable and remarkably alike. For instance, Figure **4** illustrates the similarities in the $\eta'(\omega)$ and $\eta''(\omega)$ predictions. But the similarities in the predicted behaviors of $\eta'_{13}(\omega)$, $\eta''_{13}(\omega)$, $\eta'_{33}(\omega)$ and $\eta''_{33}(\omega)$ in large-amplitude oscillatory shear flow is equally remarkable (see Figure **5** and Figure **6**).

The molecular approach does not yield explicit expressions for the constitutive equations, unless approximations such as Eqs. (19) or (21) are introduced. It may thus be useful to use an equivalent continuum model. By "equivalent" we mean that the parameters in the continuum model are so chosen that the molecular model is reasonably well approximated. The corotational model framework has been closely connected with macromolecular theory ([42,43,44]; see Tables 6.2-1 and 6.2-2 of [3]; Problems 11B.9 and 11B.10 of [29]; §IV and §V. of [28]; §9.5 of [11]). Table **I** lists examples of this procedure where the parameters of a 6-constant Oldroyd model are given for the rigid dumbbell and FENE dumbbell molecular models.

We write the stress tensor as $\boldsymbol{\tau} = \boldsymbol{\tau}_s + \boldsymbol{\tau}_p$ and the corresponding viscosities be $\eta = \eta_s + \eta_p$, and let the polymer contribution be described by the Oldroyd model; then in Table **I** we give the expressions for the six Oldroyd parameters in terms of the molecular parameters. When the rigid dumbbell parameters in Table **I** are inserted into the Oldroyd expression for viscosity or normal stresses or extensional viscosity, one will get an approximate expression for the corresponding molecular results (see p. 570-571 of [11]).

V. STEADY SHEAR FLOW

In this section, we consider the measured behavior of polymeric liquids in a time-steady simple shear flow, and the corresponding predictions for the simplest continuum and molecular models.

a. Experimental Results

For steady shear flow, the non-Newtonian viscosity $\eta(\dot\gamma) = -\tau_{yx}/\dot\gamma$ of polymers generally starts out at η_0 and then turns down and decreases more or less as $\dot\gamma^{n-1}$, with n varying from 0.2 to 0.7 for various polymeric fluids, leveling off at an infinite-shear-rate viscosity η_∞ . The first normal stress coefficient $\Psi_1 = -(\tau_{xx} - \tau_{yy})/\dot\gamma^2$ similarly begins at a constant value and then decreases more or less as $\dot\gamma^{-4/3}$. The second normal stress coefficient $\Psi_2 = -(\tau_{yy} - \tau_{zz})/\dot\gamma^2$, is generally about minus 2/7ths of the first normal coefficient (§3.2 of [3]).

b. Continuum Models

The *contravariant convected Maxwell model* gives a viscosity and a first normal stress coefficient that are both constant; it also gives *zero* for the second normal coefficient. Therefore, it is fair to say that this model is of limited value (§7.2 of [3]).

The *corotational Maxwell model* gives, for the viscosity and normal stress coefficients (see §3.2 of [29]),

$$\frac{\eta}{\eta_0} = \frac{1}{1+\left(\lambda\dot{\gamma}\right)^2}, \quad \frac{\Psi_1}{\eta_0\lambda} = -2\frac{\Psi_2}{\eta_0\lambda} = \frac{2}{1+\left(\lambda\dot{\gamma}\right)^2} \tag{25}$$

The viscosity starts at η_0 and then decreases as $\dot{\gamma}^{-2}$, which is far too steep, the largest allowable value of the exponent presumably being -1. The first normal stress coefficient decreases as $\dot{\gamma}^{-2}$ also.

If one superposes many corotational Maxwell models (see Ch 7 of [29]), with η_k and λ_k as parameters, one can then select values for these parameters according to a procedure by Winter [45] and thereby get quite realistic curves for the viscosity and first normal stress coefficient; the second normal stress coefficient is still minus one half of the first normal stress coefficient and has the opposite sign. Alternatively one can use the Spriggs relations [7], $\lambda_k = \lambda/k^\alpha$ and

$\eta_k = \eta_0 \lambda_k / \sum_k \lambda_k$ and get fairly realistic expressions with just three adjustable parameters, η_0, λ and α (see § II.a.ii above). The time constant determines the value of the shear rate at which the viscosity curve turns sharply downwards, and the parameter α controls the slope of the $\log\eta$ versus $\log\dot{\gamma}$ curve for large $\dot{\gamma}$; for example, $\eta \propto (\lambda\dot{\gamma})^{(1/\alpha)-1}$ and $\Psi_1 \propto (\lambda\dot{\gamma})^{(1/\alpha)-2}$ (see Fig. 7.4-1 of [11]).

The *corotational Jeffreys model* (Chapter 7 of [29]) decreases with shear rate and then levels off at $(\lambda_2/\lambda_1)\eta_0$ at infinite shear rate. The first normal stress coefficient decreases as $\dot{\gamma}^{-2}$, and the second normal stress coefficient is negative and has half the magnitude of the first normal stress coefficient.

We now conclude with the *ANSR model* (Arbitrary Normal Stress Ratio) [10]. This model can be regarded as a special case of the Goddard-Miller integral expansion [46] of the 8-constant Oldroyd model [16]. In steady shear flow, it gives the same results as the corotational Maxwell model for the viscosity and the first normal coefficient. However, it features an arbitrary ratio for Ψ_2/Ψ_1 that depends on an additional time constant λ_0 (see § II.b.ii above).

c. Molecular Models

The *Hookean dumbbell* (§13.4 of [8]) gives a constant viscosity, a constant first normal stress coefficient, and a second normal coefficient that is zero. This is the same prediction that is given by the Lodge "elastic liquid," which was obtained from a network model [47].

The *FENE-P dumbbell* (Example 13.5-2 of [8]) gives a non-Newtonian viscosity that has a high-shear-rate limit proportional to $\dot{\gamma}^{-2/3}$ and a high-shear-rate first normal stress coefficient proportional to $\dot{\gamma}^{-4/3}$. The second normal stress coefficient is zero.

If we *assume* that the orientational distribution function can be expanded in powers of the shear rate, then the *rigid dumbbell* gives for small shear rates ([27, 28]; §8.6 of [1]; Eqs. (14.4-18)-(14.4-20) of [8]):

$$\left(\eta\left(\dot{\gamma}\right)-\eta_s\right)/nkT\lambda = 1-\tfrac{18}{35}\left(\lambda\dot{\gamma}\right)^2+\tfrac{1326}{1925}\left(\lambda\dot{\gamma}\right)^4+\cdots \tag{26}$$

$$\Psi_1\left(\dot{\gamma}\right)/nkT\lambda^2 = \tfrac{6}{5}\left[1-\tfrac{38}{35}\left(\lambda\dot{\gamma}\right)^2+\tfrac{38{,}728}{25{,}025}\left(\lambda\dot{\gamma}\right)^4+\cdots\right] \tag{27}$$

$$\Psi_2 = 0 \tag{28}$$

However, Kim and Fan [48] have demonstrated that the above series converge only for $\lambda\dot{\gamma}$ less than about 0.8. Further, Stewart and Sørensen [49] have shown, by orthogonal collocation, that for the

limiting high shear rates

$$\left(\eta(\dot{\gamma})-\eta_s\right)/nkT\lambda \approx 0.678\left(\lambda\dot{\gamma}\right)^{-1/3} \tag{29}$$

$$\Psi_1(\dot{\gamma})/nkT\lambda^2 \approx 1.20\left(\lambda\dot{\gamma}\right)^{-4/3} \tag{30}$$

$$\Psi_2 = 0 \tag{31}$$

and Öttinger [50] has shown that the numerical coefficient in the Ψ_1 equation is $\sqrt{\pi}/2^{2/3}\Gamma\left(\frac{7}{6}\right) = 1.20357\ldots$ from his purely analytical approach. This approach takes advantage of the close alignment, at very high shear rates, of the rigid dumbbells with the flow. Then one can solve an ordinary differential equation exactly for a contracted distribution function that depends only on ϕ. However, only the numerical coefficient for Ψ_1 can be obtained in this way. Whereas Eqs. (27) and (30) are in reasonable agreement with experimental data [27], Eqs. (28) and (31) are obviously not.

The *multi-bead dumbbell* gives the same results as the rigid dumbbell, when λ is replaced by λ_N, provided that hydrodynamic interaction is neglected (see § III.b.ii above).

For the *Fraenkel dumbbell* in steady shear flow, we get exactly

$$\left(\eta_0-\eta_s\right)/nkT\lambda_H = [0,2]\zeta L^2/12kT\lambda_H = [0,2]\lambda/\lambda_H \tag{32}$$

$$\Psi_{1,0}/nkT\lambda_H^2 = [0,4]\zeta^2L^4/120k^2T^2\lambda_H^2 = \tfrac{6}{5}[0,4]\lambda^2/\lambda_H^2 \tag{33}$$

for the low-shear rate limiting values of the viscometric functions [24], where $[0,2]$ and $[0,4]$ are functions of $HL^2/2kT$, and these functions can be obtained graphically from Figs. 1(a) and 1(b) of [24] (see Problem 13B.10 of [8]).

At high shear rates (see Problem 13B.11 of [8]), we get:

$$\left(\eta(\dot{\gamma})-\eta_s\right)/nkT\lambda_H = \sqrt[3]{\tfrac{3}{2}}\left(\lambda_H\dot{\gamma}\right)^{-2/3} \tag{34}$$

$$\Psi_1(\dot{\gamma})/nkT\lambda_H^2 = \sqrt[3]{18}\left(\lambda_H\dot{\gamma}\right)^{-4/3} \tag{35}$$

In summary, all three dumbbell models that predict shear thinning (rigid, Fraenkel, FENE-P) give $\Psi_1(\dot{\gamma}) \propto (\lambda\dot{\gamma})^{-4/3}$ or $(\lambda_H\dot{\gamma})^{-4/3}$ at high shear rate. Whereas Fraenkel and FENE-P dumbbells give $(\eta(\dot{\gamma})-\eta_s) \propto (\lambda_H\dot{\gamma})^{-2/3}$ at high shear rate, the rigid dumbbell model gives $(\eta(\dot{\gamma})-\eta_s) \propto (\lambda\dot{\gamma})^{-1/3}$. Figures 3.3-1 to 3 of [3] all show the logarithm of the viscosity of polymer melts or non-dilute solutions decreasing linearly with the logarithm of the shear rate, but none of the curves has a slope of exactly $-1/3$ or $-2/3$; however, in Figure 13.5-5 of [8] the viscosity curves for non-dilute solutions have slopes very close to $-2/3$. For the first normal stress coefficient, the log-log plots *versus* shear rate in Fig. 3.3-5 of [3] for several non-dilute solutions exhibit

an extended power-law region with slopes of about -1.6 (as opposed to -1.33 of the model predictions). It should be kept in mind that by taking a mixture of dumbbells and using the Spriggs relations, we can get any desired slopes on the log-log plots of viscosity versus shear rate.

VI. SMALL-AMPLITUDE OSCILLATORY SHEAR FLOW

In this section, we consider the measured behavior of polymeric liquids in a small-amplitude oscillatory shear flow, and the corresponding predictions for the simplest continuum and molecular models.

a. Experimental Results

When the velocity gradient varies with time as $\dot{\gamma}^0 \cos\omega t$, if its amplitude is small, the shear stress and the normal stresses are then of the form (§3.4 of [3])

$$\tau_{yx}(t) = -\eta'(\omega)\dot{\gamma}^0 \cos\omega t - \eta''(\omega)\dot{\gamma}^0 \sin\omega t \tag{36}$$

$$\tau_{xx}(t) - \tau_{yy}(t) = -\left(\dot{\gamma}^0\right)^2 \left[\Psi_1^d(\omega) + \Psi_1'(\omega)\cos 2\omega t + \Psi_1''(\omega)\sin 2\omega t\right] \tag{37}$$

$$\tau_{yy}(t)-\tau_{zz}(t)=-\left(\dot{\gamma}^{0}\right)^{2}\left[\Psi_{2}^{d}(\omega)+\Psi_{2}{}'(\omega)\cos 2\omega t+\Psi_{2}{}''(\omega)\sin 2\omega t\right] \tag{38}$$

Whereas the shear stress *oscillates about zero*, but time-shifted from the input (the velocity gradient as a function of time), the two normal stress differences *oscillate about some constant* which depends on the displacement functions Ψ_1^d and Ψ_2^d. Thus, the two η functions and six Ψ functions are the experimentally measurable quantities.

There are two important empirical rules connecting small-amplitude oscillatory functions with steady shear flow functions (§3.6 of [3]; [51, 52]):

Cox-Merz rule: $$\eta(\dot{\gamma})=\left|\eta^{*}(\omega)\right|_{\omega=\dot{\gamma}}=\eta'(\omega)\left[1+\left(\eta''/\eta'\right)^{2}\right]^{0.5}\Big|_{\omega=\dot{\gamma}} \tag{39}$$

Laun rule: $$\Psi_{1}(\dot{\gamma})=\left(2\eta''(\omega)/\omega\right)\left[1+\left(\eta''/\eta'\right)^{2}\right]^{0.7}\Big|_{\omega=\dot{\gamma}} \tag{40}$$

These relations can be useful if steady state flow data are not available, but small-amplitude oscillatory data are at hand.

b. Continuum Models

The two-constant *contravariant convected Maxwell model* gives, for η' and η'' (Table 3 of [27]),

$$\eta'(\omega)/\eta_{0}=1/\left[1+(\lambda\omega)^{2}\right]=1-(\lambda\omega)^{2}/\left[1+(\lambda\omega)^{2}\right] \tag{41}$$

$$\eta''(\omega)/\eta_0 = \lambda\omega/\left[1+(\lambda\omega)^2\right] \tag{42}$$

These functions show the general trends, namely that η' and $\eta''/\lambda\omega$ both decrease with increasing frequency. For describing experimental data, one can superpose Maxwell models and get

$$\eta'(\omega) = \sum_j \eta_j/\left[1+(\lambda_j\omega)^2\right] = \sum_j \eta_j\left(1-(\lambda_j\omega)^2/\left[1+(\lambda_j\omega)^2\right]\right) \tag{43}$$

$$\eta''(\omega) = \sum_j \eta_j\lambda_j\omega/\left[1+(\lambda\omega)^2\right] \tag{44}$$

One can then use Winter's method [45] for selecting 20 or 30 η_j and λ_j to get excellent fits of the experimental data. Alternatively one can use the Spriggs relations [7] and get 3-parameter descriptions of the experimental data (see § II.a.ii above).

The *corotational Maxwell* model gives exactly the same results as the contravariant convected Maxwell model (Example 7.3-2 of [11]). The *three-constant corotational Jeffreys* model (Example 7.3-2 of [11]) gives for η' and η'':

$$\eta'(\omega)/\eta_0 = (1+\lambda_1\lambda_2)/\left[1+(\lambda_1\omega)^2\right] = 1-\left[(\lambda_1\omega)^2-\lambda_1\lambda_2\right]/\left[1+(\lambda_1\omega)^2\right] \tag{45}$$

$$\eta''(\omega)/\eta_0 = (\lambda_1-\lambda_2)\omega/\left[1+(\lambda_1\omega)^2\right] \tag{46}$$

This result can be used to superimpose many Jeffreys models. We can do this by replacing λ_1 by $\lambda_{1k} = \lambda/k^\alpha$ and λ_2 by $\lambda_{2k} = \lambda/k^\alpha$ in Eqs. (7) , and using the same value of *k* and α appearing in both

expressions. Thus we still end up with a three-parameter description of the experimental data." (see § II.a.ii above).

The linear viscoelastic functions for the *ANSR model* are the same as for the corotational Maxwell model.

c. Molecular Models

The *Hookean dumbbell* gives, for the linear viscoelastic functions (§13.4 of [8])

$$\left(\eta'(\omega)-\eta_s\right)/nkT\lambda_H = 1/\left[1+\left(\lambda_H\omega\right)^2\right] = 1-\left(\lambda_H\omega\right)^2/\left[1+\left(\lambda_H\omega\right)^2\right] \tag{47}$$

$$\eta''(\omega)/nkT\lambda_H = \lambda_H\omega/\left[1+\left(\lambda_H\omega\right)^2\right] \tag{48}$$

This gives the right general trends for the functions, but is not adequate for describing the experimental data exactly. Superposing the Hookean dumbbells, however, gives excellent results. The *FENE-P dumbbell* gives the same results as the Hookean dumbbell.

The *rigid dumbbell* gives, for small-amplitude oscillatory shear flow (§7 of [27]),

$$\left(\eta'(\omega)-\eta_s\right)/nkT\lambda = \left[1+\tfrac{2}{5}\left(\lambda\omega\right)^2\right]/\left[1+\left(\lambda\omega\right)^2\right] = 1-\tfrac{3}{5}\left(\lambda\omega\right)^2/\left[1+\left(\lambda\omega\right)^2\right] \tag{49}$$

$$\eta''(\omega)/nkT\lambda = \tfrac{3}{5}\lambda\omega/\left[1+\left(\lambda\omega\right)^2\right] \tag{50}$$

Though these differ from Eqs. (47) and (48), they give the same general trends for the functions. Whereas Eqs. (47) and (48) intersect (at $\lambda_H \omega = 1$), Eqs. (49) and (50) give $\eta'(\omega) > \eta''(\omega)$ everywhere. This intersection of η'' with η' is sometimes observed (see Figure 9-22 of [53], and sometimes, not (see Figures 9-1 and 9-3 of [53]).

The *multi-bead rod* gives the same results as for the rigid dumbbell, except that λ is replaced by λ_N, provided that hydrodynamic interaction is not taken into account (see § III.b.ii above).

We know of no analytical solution for the *Fraenkel dumbbell* in small-amplitude oscillatory shear flow, although Fraenkel has given approximate results for three special cases (see p. 646, Column 2, entries (1) through (3) of [23]).

For the *Rouse chain* we get (Eqs. (15.3-29) and (15.3-29) of [8]):

$$\begin{aligned}\left(\eta'(\omega) - \eta_s\right)/nkT\lambda_R &= \left(1/\lambda_R\right)\sum_j^{N-1} \lambda_j \Big/ \left[1 + \left(\lambda_j\omega\right)^2\right] \\ &= \left(1/\lambda_R\right)\sum_j^{N-1} 1 - \left[1 + \left(\lambda_j\omega\right)^2 - \lambda_j\right] \Big/ \left[1 + \left(\lambda_j\omega\right)^2\right]\end{aligned} \tag{51}$$

$$\eta''(\omega)/nkT\lambda_R = \left(1/\lambda_R\right)\sum_j^{N-1} \lambda_j^2\omega \Big/ \left[1 + \left(\lambda_j\omega\right)^2\right] \tag{52}$$

Comparing these with Eqs. (43) and (44) for the contravariant convected Maxwell model, we see that if we neglect the solvent viscosity, we can then identify η_j with the constants $nkT\lambda_j$.

VII. STEADY EXTENSIONAL FLOW

In this section, we consider the measured behavior of polymeric liquids in a steady extensional flow, and the corresponding predictions for the simplest continuum and molecular models.

a. Experimental Results

For steady extensional flow, the quantity that is measured is the extensional viscosity $\bar{\eta}(\dot{\varepsilon}) = -(\tau_{zz} - \tau_{xx})/\dot{\varepsilon}$, which depends upon the extension rate $\dot{\varepsilon} = dv_z/dz$. For Newtonian fluids, the extensional viscosity is three times the viscosity μ. For some polymeric fluids, the extensional viscosity is $3\eta_0$ for small values of $\dot{\varepsilon}$, and, as $\dot{\varepsilon}$ increases, $\bar{\eta}$ increases somewhat, goes through a maximum, and then decreases. For others, no maximum is observed. And for still others, it is not possible to achieve a steady-state flow.

For negative $\dot{\varepsilon}$ (biaxial stretching), $\bar{\eta}$ decreases and seems to go to a constant, although the experimental data for this are very limited (§8.2 of [1]).

b. Continuum Models

The *contravariant convected Maxwell model* gives, for the extensional viscosity (Table 7.3-2 of [3]),

$$\bar{\eta}(\dot{\varepsilon})/3\eta_0 = 1/(1+\lambda\dot{\varepsilon})(1-2\lambda\dot{\varepsilon}) \tag{53}$$

which gives infinity for $\lambda\dot{\varepsilon} \geq \frac{1}{2}$ and $\lambda\dot{\varepsilon} \leq -1$. Whereas some regard this as unacceptable, some process engineers use this to explain maximum throughput in extensional manufacturing flows such as fiber spinning (where $\lambda\dot{\varepsilon} > 0$) or film blowing (where $\lambda\dot{\varepsilon} < 0$).

The *corotational Maxwell* and *Jeffreys models* both give, for the extensional viscosity (Chapter 7 of [3]),

$$\bar{\eta}(\dot{\varepsilon})/3\eta_0 = 1 \tag{54}$$

This result does not give rise to any infinities, but it does not leave room for any flexibility.

To our knowledge, no one has previously evaluated the extensional viscosity for the *ANSR model,* for which we get*:*

$$\bar{\eta}/3\eta_0 = 1 + \lambda_0\dot{\varepsilon} \tag{55}$$

a reasonable result for positive $\lambda_0\dot{\varepsilon}$, but not for $\lambda_0\dot{\varepsilon} \leq -1$.

c. Molecular Models

The *Hookean dumbbell* gives, for the extensional viscosity (Table 3 of [27]),

$$\left(\bar{\eta}\left(\dot{\varepsilon}\right)-3\eta_s\right)/3nkT\lambda_H = 1/\left(1+\lambda_H\dot{\varepsilon}\right)\left(1-2\lambda_H\dot{\varepsilon}\right) \tag{56}$$

which suffers from the same fundamental weaknesses that the contravariant convected Maxwell model does.

For the *FENE-P dumbbells*, we have the following results for extensional flow (Example 13.5-2(d) of [3])

For $\dot{\varepsilon}=0$: $\left(\bar{\eta}\left(\dot{\varepsilon}\right)-3\eta_s\right)/3nkT\lambda_H = b/\left(b+5\right)$ (57)

For $\dot{\varepsilon}\to\infty$: $\left(\bar{\eta}\left(\dot{\varepsilon}\right)-3\eta_s\right)/3nkT\lambda_H \cong \frac{2}{3}b$ (58)

For $\dot{\varepsilon}\to-\infty$: $\left(\bar{\eta}\left(\dot{\varepsilon}\right)-3\eta_s\right)/3nkT\lambda_H \cong \frac{1}{6}b$ (59)

These results show that the nonlinear spring in this model prevents the infinities from occurring.

For *rigid dumbbells* it can be shown that (Example 14.4-2 of [8]; Eq. (16.5) of [27])

$$\begin{aligned}\left(\bar{\eta}\left(\dot{\varepsilon}\right)-3\eta_s\right)/3nkT\lambda &= \tfrac{1}{2}\mp\tfrac{3}{4}X\pm\tfrac{3}{4}\sqrt{X}\exp\left(\pm\mathrm{X}\right)\Big/\int_0^{\sqrt{X}}\exp\left(\pm y\right)dy \\ &= 1+\tfrac{3}{5}\lambda\dot{\varepsilon}+\tfrac{9}{35}\left(\lambda\dot{\varepsilon}\right)^2-\tfrac{27}{175}\left(\lambda\dot{\varepsilon}\right)^3+\cdots\end{aligned} \tag{60}$$

in which $X=\frac{9}{2}\lambda\left|\dot{\varepsilon}\right|$ and the upper signs are to be used when $\dot{\varepsilon}$ is positive and the lower signs, when $\dot{\varepsilon}$ is negative. This monotone

increasing function of $\dot{\varepsilon}$, $\left(\bar{\eta}\left(\dot{\varepsilon}\right)-3\eta_s\right)/3nkT\lambda$, ranges from $\frac{1}{2}$ to 2 as $\dot{\varepsilon}$ increases from $-\infty$ to $+\infty$. This seems not altogether unreasonable.

The results for the *multi-bead rod* match those for the rigid dumbbell, if λ is replaced by λ_N.

For the Kramers *freely jointed bead rod chain*, Hassager ([33]; §16.5 of [8]) has succeeded in developing series expansions for both small and large rates of extension. He has compared his results with those for multi-bead rods. In the limits of $\dot{\varepsilon}$ going to plus or minus infinity, the two curves have common asymptotes.

VIII. LARGE-AMPLITUDE OSCILLATORY SHEAR FLOW

In this section, we consider the measured behavior of polymeric liquids in a large-amplitude oscillatory shear flow, and the corresponding predictions for the simplest continuum and molecular models.

If the amplitude $\dot{\gamma}^0$ of the velocity gradient $\dot{\gamma}^0\cos\omega t$ is large, then harmonics higher than those given by Eqs. (36) through (38) are measured. These higher harmonics distort the stress responses, and when we observe these in the shear stress response, we call the

oscillatory experiment *large-amplitude*. For polymeric liquids, these higher harmonics are commonly observed when:

$$\frac{\omega}{\dot{\gamma}^0} > 1 \tag{61}$$

Eq. (61) is thus our working definition of large-amplitude oscillatory shear flow [54,55], and with recent advances in rheometry, conducting experiments satisfying Eq. (61) is now commonplace for exploring the physics of polymeric liquids [56]. The material functions in this flow are commonly defined as coefficients of the Fourier series [compare with Eqs. (36) to (38)]:

$$\frac{\tau_{yx}\left(t,\gamma_0\right)}{\dot{\gamma}^0} \equiv -\sum_{\substack{h=1 \\ \text{odd}}}^{\infty} \eta'_h\left(\omega,\dot{\gamma}^0\right)\cos h\omega t + \eta''_h\left(\omega,\dot{\gamma}^0\right)\sin h\omega t \tag{62}$$

$$\frac{\tau_{xx}\left(t\right)-\tau_{yy}\left(t\right)}{\left(\dot{\gamma}^0\right)^2} \equiv -\sum_{\substack{h=0 \\ \text{even}}}^{\infty} \Psi'_{1,h}\left(\omega,\dot{\gamma}^0\right)\cos h\omega t + \Psi''_{1,h}\left(\omega,\dot{\gamma}^0\right)\sin h\omega t \tag{63}$$

$$\frac{\tau_{yy}\left(t\right)-\tau_{zz}\left(t\right)}{\left(\dot{\gamma}^0\right)^2} \equiv -\sum_{\substack{h=0 \\ \text{even}}}^{\infty} \Psi'_{2,h}\left(\omega,\dot{\gamma}^0\right)\cos h\omega t + \Psi''_{2,h}\left(\omega,\dot{\gamma}^0\right)\sin h\omega t \tag{64}$$

where h is the order of the harmonic, and where $\Psi'_{1,0} = \Psi'^{\,d}_1$, $\Psi''_{1,0} = \Psi''^{d}_1$, $\Psi'_{2,0} = \Psi'^{\,d}_2$ and $\Psi''_{2,0} = \Psi''^{d}_2$. We call the coefficients, $\eta'_h\left(\omega,\dot{\gamma}_0\right)$ and $\eta''_h\left(\omega,\dot{\gamma}^0\right)$, the *Fourier loss and storage viscosities of the hth harmonic*. Mindful of our errata to our Ref. [17], we see that the

notation corresponding to Eq. (62), for the first normal stress difference coefficient is given in Eq. (179) of [17]. These Fourier viscosities are also readily obtained from loops, such as the one in Figure **3** [57].

The Fourier viscosities in Eq. (62) are occasionally expanded in odd powers of $\dot{\gamma}_0$ thus defining a matrix of frequency dependent nonlinear viscosities [58]:

$$\frac{\tau_{yx}(t)}{\dot{\gamma}_0} = -\sum_{\substack{n=1 \\ \text{odd}}}^{\infty} \sum_{\substack{h=1 \\ \text{odd}}}^{n} \dot{\gamma}^{0\,n-1} \left[\eta'_{hn}(\omega) \cos h\omega t + \eta''_{hn}(\omega) \sin h\omega t \right] \tag{65}$$

where $(\eta'_{hn}, \eta''_{hn})$ are named the *loss and storage viscosities of hn*th *order*, where $(\eta'_{11}, \eta''_{11}) \equiv (\eta', \eta'')$. The "*n*" in the "*hn*th order" corresponds to *one plus* the power of the expansion in Eq. (65), that is, the power of $\dot{\gamma}^0$ in in Eq. (65). Whereas the Fourier viscosities all have the same dimensions, of viscosity, the dimensions of the viscosities of *hn*th order are given by:

$$(\eta'_{hn}, \eta''_{hn}) [=] \frac{(\eta', \eta'')}{\dot{\gamma}^{0\,n-1}} \tag{66}$$

The notation corresponding to Eq. (65), for the first normal stress differences, is (Eq. (183) of [17]):

$$\frac{\tau_{xx}(t)-\tau_{yy}(t)}{\eta_0\dot{\gamma}^0} = -\sum_{\substack{p=1\\ \text{odd}}}^{\infty}\sum_{\substack{h=0\\ \text{even}}}^{p+1}\dot{\gamma}^{0\,p}\left[\Psi'_{1,h,p+2}(\omega)\cos h\omega t + \Psi''_{1,h,p+2}(\omega)\sin h\omega t\right] \tag{67}$$

defining a matrix of frequency dependent nonlinear coefficients.

The latest addition to LAOS notation is [59,60]:

$$\frac{\tau_{yx}(\tau,\dot{\gamma}_0)}{\dot{\gamma}_0} \equiv \sum_{\substack{n=1\\ \text{odd}}}^{\infty}\frac{G_{En}}{\omega}(\omega,\dot{\gamma}_0)T_n\sin\omega t + \sum_{\substack{n=1\\ \text{odd}}}^{\infty}\eta_{En}(\omega,\dot{\gamma}_0)T_n\cos\omega t \tag{68}$$

where $T_n(x)$ are the Tschebycheff polynomials of the first kind, for which:

$$T_{n+1}(x) \equiv 2xT_n(x) - T_{n-1}(x); T_0(x) \equiv 1 \tag{69}$$

We call $G_{En}(\omega,\dot{\gamma}_0)$ the Ewoldt moduli and and $\eta_{En}(\omega,\dot{\gamma}_0)$, the Ewoldt viscosities. These Ewoldt coefficients are related to the Fourier coefficients in (62) by [61]:

$$G_{En}(\omega,\dot{\gamma}_0) = \eta''_n(\omega,\dot{\gamma}_0)(-1)^{(n-1)/2} \tag{70}$$

$$\eta_{En}(\omega,\dot{\gamma}_0) = \eta'_n(\omega,\dot{\gamma}_0)/\omega \tag{71}$$

When shear stress shear rate loops self-intersect, they form *secondary loops* [64], and these have been shown to arise when [61]:

$$\frac{G_{E3}}{G_{E1}} > \frac{1}{3}\left(1+5\frac{G_{E5}}{G_{E1}}-\cdots\right) \tag{72}$$

As for self-intersection in large-amplitude oscillatory shear flow, none of the solutions to simple models explored in this review have been tested against Eq. (72). For self-intersection, a more complicated corotational continuum model has been proposed [62] which exploits the Gordon-Schowalter derivative [63].

a. Experimental Results

To evaluate constitutive equations, we rely on experimental measurements. In rheology, these are collected as time series, usually $\tau_{yx}(t)$ and very rarely as $\left[\tau_{xx}(t)-\tau_{yy}(t)\right]$ [10,83,84]. The Fourier viscosities in Eqs. (65) and (67) are readily obtained from measured time series $\tau_{yx}(t)$ using the discrete Fourier transform [55]. Many then follow Dealy *et al.* (1973) in plotting loops of shear stress versus shear rate, since these best bring out distortions from ellipticity caused by the higher harmonics [64,65,66]. The oscillograph in Figure 3, for example, shows why putting $\dot{\gamma}$ on the abscissa is preferred for detecting higher harmonic content. This measurement was made on a sliding plate rheometer incorporating a flush-mounted shear stress transducer [67,68].

Recent experimental work focuses on the ratios of the amplitudes of harmonics (particularly the third-to-first and fifth-to-first), often called the *relative intensities*, a now widely established way of representing large-amplitude oscillatory shear measurements (see Fig. 2 of [69]; see Fig. 4.12 of [70,71]; see Fig. 6 of [72]). The *shear stress harmonic amplitude* is defined by:

$$\left|\tau_h\right| = \dot{\gamma}^0 \sqrt{\eta_h'^2 + \eta_h''^2} \tag{73}$$

This concept of relative intensities follows naturally from the analysis of molecular spectroscopy [70], and has become a popular way of summarizing nonlinear viscoelastic behavior. The symbols $I_{3/1}$ and $I_{5/1}$ are often used for the amplitude ratios, $\left|\tau_3\right|/\left|\tau_1\right|$ and $\left|\tau_5\right|/\left|\tau_1\right|$, and:

$$\lim_{\left(\dot{\gamma}^0/\omega\right)\to 0} \frac{\left|\tau_3\right|/\left|\tau_1\right|}{\left(\dot{\gamma}^0/\omega\right)^2} \equiv Q_0^{3/1} \tag{74}$$

$$\lim_{\left(\dot{\gamma}^0/\omega\right)\to 0} \frac{\left|\tau_5\right|/\left|\tau_1\right|}{\left(\dot{\gamma}^0/\omega\right)^4} \equiv Q_0^{5/1} \tag{75}$$

where $\left(\dot{\gamma}^0/\omega\right)$ is called the shear strain amplitude. $Q_0^{3/1}$ is called the *intrinsic nonlinearity* (for a thorough treatment of this quantity see [73]). Since $Q_0^{3/1}$ is measured at constant frequency, Eqs. (74) and (75) become:

$$Q_0^{3/1} = \omega^2 \lim_{\dot{\gamma}^0 \to 0} \frac{\left|\boldsymbol{\tau}_3\right| / \left|\boldsymbol{\tau}_1\right|}{\left(\dot{\gamma}^0\right)^2} = \left(\lambda\omega\right)^2 \lim_{\dot{\gamma}^0 \to 0} \frac{\left|\boldsymbol{\tau}_3\right| / \left|\boldsymbol{\tau}_1\right|}{\left(\lambda\dot{\gamma}^0\right)^2} \tag{76}$$

$$Q_0^{5/1} = \omega^2 \lim_{\dot{\gamma}^0 \to 0} \frac{\left|\boldsymbol{\tau}_3\right| / \left|\boldsymbol{\tau}_1\right|}{\left(\dot{\gamma}^0\right)^4} = \left(\lambda\omega\right)^4 \lim_{\dot{\gamma}^0 \to 0} \frac{\left|\boldsymbol{\tau}_3\right| / \left|\boldsymbol{\tau}_1\right|}{\left(\lambda\dot{\gamma}^0\right)^4} \tag{77}$$

These limits are thus inspired by the usual expansions for the steady shear viscosity, or for the shear stress response in large-amplitude oscillatory shear, which generally give power-laws (see Eq. (9) of [74] and Eq. (3) of [75]; see Eq. (5) of [76]; see Eq. (13) of [77] and Eq. (17) of [78]]; see Eqs. (147) and (157) of [17]; see Eq. (3) of [69]; [79,80,81]):

$$\left|\boldsymbol{\tau}_h\right| / \left|\boldsymbol{\tau}_1\right| \propto \left(\dot{\gamma}^0\right)^{h-1} ; h > 1, \text{odd} \tag{78}$$

where h is the integer order of the harmonic, and specifically:

$$\begin{aligned} \left|\boldsymbol{\tau}_3\right| / \left|\boldsymbol{\tau}_1\right| &\propto \left(\dot{\gamma}^0\right)^2 \\ \left|\boldsymbol{\tau}_3\right| / \left|\boldsymbol{\tau}_1\right| &\propto \left(\dot{\gamma}^0\right)^4 \end{aligned} \tag{79}$$

The power-laws given by Eq. (78), and especially the first one, by Eq. (79), are often confirmed experimentally [82]. Finally, whereas loop self-intersection has been measured [65,66], Eq. (72) has yet to be evaluated for any of the simple models considered in this review.

b. Continuum Models

The *contravariant convected Maxwell* model gives, for the shear stress and the normal stress differences, for a cosinusoidal velocity gradient $\dot{\gamma}^0 \cos \omega t$, once alternance is reached

$$\frac{\tau_{yx}(t)}{\eta_0 \dot{\gamma}^0} = -\frac{1}{1+(\lambda\omega)^2}\left(\cos \omega t + \lambda\omega \sin \omega t\right) \tag{80}$$

$$\frac{\tau_{xx}(t)-\tau_{yy}(t)}{\eta_0 \dot{\gamma}^0} = -\lambda\dot{\gamma}^0\left[\frac{1}{1+(\lambda\omega)^2} + \frac{\left(1-2(\lambda\omega)^2\right)\cos 2\omega t + 3\lambda\omega \sin 2\omega t}{\left(1+(\lambda\omega)^2\right)\left(1+4(\lambda\omega)^2\right)}\right] \tag{81}$$

$$\tau_{yy}(t)-\tau_{zz}(t) = 0 \tag{82}$$

By *alternance* we mean that initial transients have disappeared. Mindful of the errata in our Ref. [47], we see that Eqs. (80) and (81) match Eqs. (6.40) and (6.41) of [47] (see Appendix B of [83]; [84, 85]). Whereas the shear stress oscillates at the shear-rate frequency, the first normal stress difference oscillates about a negative average value, with double the shear-rate frequency. Thus, only zeroth, first and second harmonics are involved in the large-amplitude flows. Comparing Eq. (80) with (65), we see that $\eta'(\omega) = \eta_1'(\omega) = \eta_0 \Big/ \left[1+(\lambda\omega)^2\right]$

and $\eta''(\omega)=\eta_1''(\omega)=\eta_0\dot{\gamma}^0\lambda\omega\Big/\left[1+(\lambda\omega)^2\right]$, and comparing Eq. (81) with (63), that $\Psi'_{1,0}=\Psi_1^d(\omega)=\lambda\eta'(\omega)$.

The *corotational Maxwell model* behaves quite differently, following the patterns of Eqs. (65) and (67). Here it is found that, once alternance is reached (Eqs. (58) and (66) of [9])

$$\begin{aligned}\frac{\tau_{yx}(t)}{\dot{\gamma}^0}=&-\left[\eta'_{11}(\omega)\cos\omega t+\eta''_{11}(\omega)\sin\omega t\right]\\&-\dot{\gamma}^{0\,2}\begin{bmatrix}\eta'_{13}(\omega)\cos\omega t+\eta''_{13}(\omega)\sin\omega t\\+\eta'_{33}(\omega)\cos 3\omega t+\eta''_{33}(\omega)\sin 3\omega t\end{bmatrix}\\&-\dot{\gamma}^{0\,4}\begin{bmatrix}\eta'_{15}(\omega)\cos\omega t+\eta''_{15}(\omega)\sin\omega t\\+\eta'_{35}(\omega)\cos 3\omega t+\eta''_{35}(\omega)\sin 3\omega t\\+\eta'_{55}(\omega)\cos 5\omega t+\eta''_{55}(\omega)\sin 5\omega t\end{bmatrix}\\&-\cdots\end{aligned}\tag{83}$$

$$\frac{\tau_{xx}-\tau_{yy}}{\eta_0\dot{\gamma}^0}=-2\frac{\tau_{yy}-\tau_{zz}}{\eta_0\dot{\gamma}^0}=-\dot{\gamma}^0\begin{bmatrix}+\dot{\gamma}^{0\,0}\left(\Psi'_{1,01}+\Psi'_{1,21}\cos 2\omega t+\Psi''_{1,21}\sin 2\omega t\right)\\+\dot{\gamma}^{0\,2}\begin{pmatrix}\Psi'_{1,03}+\Psi'_{1,23}\cos 2\omega t+\Psi''_{1,23}\sin 2\omega t\\+\Psi'_{1,43}\cos 4\omega t+\Psi''_{1,43}\sin 4\omega t\end{pmatrix}\\+\cdots\end{bmatrix}\tag{84}$$

in which the functions (η'_{hn},η''_{hn}) and $\left(\Psi'_{1,h,p+2},\Psi''_{1,h,p+2}\right)$, which depend only on $\lambda\omega$, are given in Eqs. (160) through (171) and Eqs. (186) through (193) of [9]. In Eqs. (83) and (84), mindful of our errata to Eq. (66) after Ref. [9]), we see that all coefficients of the sine functions, $\left(\eta''_{mn},\Psi''_{1,h,p+2}\right)$ contain a factor of $\lambda\omega$. (see Eqs. (58) and (66) of [9].

Alternatively, a tidy, compact, unique, *exact* solution for this same corotational Maxwell model in large-amplitude oscillatory shear has recently been given [86]:

$$\frac{\tau_{yx}}{\eta_0\dot{\gamma}^0} = -\left(e^{-t/\lambda}/\lambda\omega\right)\left[\sin\left(\left[\dot{\gamma}^0/\omega\right]\sin\omega t\right)I_1 + \cos\left(\left[\dot{\gamma}^0/\omega\right]\sin\omega t\right)I_2\right] \tag{85}$$

$$\frac{\tau_{xx}-\tau_{yy}}{\eta_0\dot{\gamma}^0} = \left(2e^{-t/\lambda}/\lambda\omega\right)\left[\cos\left(\left[\dot{\gamma}^0/\omega\right]\sin\omega t\right)I_1 - \sin\left(\left[\dot{\gamma}^0/\omega\right]\sin\omega t\right)I_2\right] \tag{86}$$

$$\frac{\left(\tau_{yy}-\tau_{zz}\right)}{\eta_0\dot{\gamma}^0} = -\left(e^{-t/\lambda}/\lambda\omega\right)\left[\cos\left(\left[\dot{\gamma}^0/\omega\right]\sin\omega t\right)I_1 - \sin\left(\left[\dot{\gamma}^0/\omega\right]\sin\omega t\right)I_2\right] \tag{87}$$

where the functions $I_1\left(\dot{\gamma}^0/\omega\right)$ and $I_2\left(\dot{\gamma}^0/\omega\right)$ are given in "Appendix: I_1, I_2, and Their Limits" of [86]. Eqs. (85) through (87) have been used to confirm the accuracy of Eqs. (83) and (84). To our knowledge, Eqs. (85) through (87) are the only exact solution for large-amplitude oscillatory shear flow where the material responses contain higher harmonics. Eqs. (83) and (84) have also been improved upon with ratios of polynominals, called Padé approximants [87].

For the corotational Maxwell model, Eq. (83) yields (from Eq. (45) and (46) of [82]):

$$\frac{\left|\tau_3\right|}{\left|\tau_1\right|} = \frac{Q_0^{3/1}}{\left(\lambda\omega\right)^2} = \frac{\sqrt{\left(1-11W\right)^2+36W\left(1-W\right)^2}}{4\left(1+4W\right)\left(1+9W\right)\sqrt{1+W^2}}\left(\lambda\dot{\gamma}^0\right)^2 - \cdots \tag{88}$$

$$\frac{|\tau_5|}{|\tau_1|} = \frac{Q_0^{5/1}}{(\lambda\omega)^4} = \frac{\sqrt{(1-85W+274W^2)^2 + W(15-225W+120W^2)^2}}{16(1+W)(1+4W)(1+9W)(1+16W)(1+25W)\sqrt{1+W^2}}(\lambda\dot{\gamma}^0)^4 - \cdots \tag{89}$$

where $W = (\lambda\omega)^2$. Eqs. (88) and (89) which, to leading order, match the first and second power-laws of large-amplitude oscillatory shear flow given by Eqs. (79) [82].

The *corotational Jeffreys model* gives a somewhat different result from the corotational Maxwell model (see Section 8 of [9]). The *ANSR model* gives exactly the same results as Eqs. (83) and (84), the results for the corotational Maxwell model for shear stress and the first normal stress difference. However, it does give the opportunity to alter the second normal stress differences by a factor [17, 18]. The ANSR model is the special case of the Oldroyd 8-constant model omitting all parameters except η_0, λ_1, and μ_1.

c. Molecular Models

The *Hookean dumbbell* gives the same results as for the contravariant convected Maxwell model, Eq. (4), except for the Newtonian solvent contribution. Large-amplitude oscillatory shear

flow has not been published for the *FENE-P dumbbell*, as far as we know.

Recently, there have been several publications dealing with the shear and normal stress responses of suspensions of *rigid dumbbells* in large-amplitude oscillatory shearing motion. One must first get the orientational distribution function by solving a partial differential equation as a power series in $\lambda_H \dot{\gamma}^0$ (§ II.9. of [27]; [88,89,90,91]). Bird and Armstrong [92] established a method for calculating the shear stress and normal stress responses to any simple shear flow (see also Problem 11C.1 of [29]) for a dilute solution of rigid dumbbells without hydrodynamic interaction. This method has been used to analyze small-amplitude oscillatory shear flow in gaps with dimensions similar to that of the dumbbells (see Section 5. of [93]; Section 2.3.3 of [94]).

Then the shear stress and first normal stress responses follow the patterns of Eqs. (65) and (67) [95]

$$\frac{\tau_{yx}-\tau_{yx,s}}{nkT\left(\lambda\dot{\gamma}^0\right)}=-\frac{1}{nkT\lambda}\begin{bmatrix}\eta'_{11}(\omega)\cos\omega t+\eta''_{11}(\omega)\sin\omega t\\ -\dot{\gamma}^{0\,2}\begin{pmatrix}\eta'_{13}(\omega)\cos\omega t+\eta''_{13}(\omega)\sin\omega t\\ +\eta'_{33}(\omega)\cos 3\omega t+\eta''_{33}(\omega)\sin 3\omega t\end{pmatrix}\\ -\cdots\end{bmatrix} \tag{90}$$

$$\frac{\tau_{xx}-\tau_{yy}}{\eta_0\left(\dot{\gamma}^0\right)^2}=-\frac{1}{nkT\lambda^2}\begin{bmatrix}\dot{\gamma}^{0\,0}\left(\Psi'_{1,01}+\Psi'_{1,21}\cos 2\omega t+\Psi''_{1,21}\sin 2\omega t\right)\\ +\dot{\gamma}^{0\,2}\begin{pmatrix}\Psi'_{1,03}+\Psi'_{1,23}\cos 2\omega t+\Psi''_{1,23}\sin 2\omega t\\ +\Psi'_{1,43}\cos 4\omega t+\Psi''_{1,43}\sin 4\omega t\end{pmatrix}\\ +\cdots\end{bmatrix} \tag{91}$$

$$\frac{\tau_{yy}-\tau_{zz}}{\eta_0\left(\dot{\gamma}^0\right)^2}=-\frac{1}{nkT\lambda^2}\begin{bmatrix}\dot{\gamma}^{0\,0}\left(0+\Psi'_{2,21}\cos 2\omega t+\Psi''_{2,21}\sin 2\omega t\right)\\ +\dot{\gamma}^{0\,2}\begin{pmatrix}\Psi'_{2,03}+\Psi'_{2,23}\cos 2\omega t+\Psi''_{2,23}\sin 2\omega t\\ +\Psi'_{2,43}\cos 4\omega t+\Psi''_{2,43}\sin 4\omega t\end{pmatrix}\\ +\cdots\end{bmatrix} \tag{92}$$

where $nkT\lambda$ is identified with the dumbbell contribution to the zero-shear-rate viscosity, $\eta_0-\eta_s$. In Eqs. (90) and (91), η'_{hn}, η''_{hn}, $\Psi'_{1,hn}$, $\Psi''_{1,hn}$, $\Psi'_{2,hn}$ and $\Psi''_{2,hn}$ depend only on $\lambda\omega$; η'_{hn} and η''_{hn} are given in Eqs. (90) through (95) of [88], $\Psi'_{1,hn}$ and $\Psi''_{1,hn}$ in Eqs. (15) through (19) and $\Psi'_{2,hn}$ and $\Psi''_{2,hn}$ in Eqs. (23) through (27) of [90]. Though these functions differ from those given for the corotational Maxwell model [Eqs. (83) and (84)], the qualitative behaviors of η'_{hn}, η''_{hn}, $\Psi'_{1,hn}$ and $\Psi''_{1,hn}$ do not differ (see Figures 6 through 8 of [88]). Further, all coefficients of the sine functions, $\left(\eta''_{mn},\Psi''_{1,hn},\Psi''_{2,hn}\right)$ contain the factor $\lambda\omega$. Whereas Eqs. (90) and (91) are of the form of Eqs. (83) and (84), Eq. (92) differs strikingly from Eq. (84) by its zero $\Psi'_{2,01}$. In other

words, for the molecular theory, the second normal stress difference oscillates about zero.

For the *multi-bead rod*, the results for the rigid dumbbell can be taken over directly if λ is replaced by λ_N, if hydrodynamic interaction is neglected (see § III.b.ii above).

IX. NON-ISOTHERMAL FLOWS

For incompressible, non-isothermal flow problems, in addition to the equation of motion, Eq. (1), we need the energy equation

$$\rho\hat{C}_p\frac{DT}{Dt} = -\left(\nabla\cdot\mathbf{q}\right) - \left(\boldsymbol{\tau}:\nabla\mathbf{v}\right) \tag{93}$$

in which $\mathbf{q}$ is the heat-flux vector, and $-\left(\boldsymbol{\tau}:\nabla\mathbf{v}\right)$ gives the irreversible transformation of mechanical energy into thermal energy, commonly called *viscous heating*. Then, using the general expressions for the Fourier series for the shear stress response, Eq. (62), general expressions for the temperature rise in oscillatory shear flow have been explored analytically [96]. From these we learn that the temperature rise will oscillate significantly about its average value, at even multiples of the test frequency, ω, and that the coefficients of

the higher harmonics in Eq. (62) influence the amplitudes of these even harmonics of the temperature rise.

For any continuum model, whose behavior conforms to Eqs. (41) and (42), expressions for the temperature rise in small-amplitude oscillatory shear flow exist (see Eq. (51) of [97]). The temperature rise in large-amplitude oscillatory shear flow, specific to a corotational Maxwell fluid, has also been explored analytically [98]. By contrast, the temperature rise for molecular models in oscillatory shear flow has yet to be explored. This would require the expression for the shear stress response in oscillatory shear flow to be combined with Eq. (8) of [98]. For instance, for the suspension of rigid dumbbells, we would combine Eq. (49) with Eq. (8) of [98] to get the temperature rise in small-amplitude oscillatory shear flow, and Eq. (90) with Eq. (8) of [98] for large-amplitude. In oscillatory shear flow, be it large or small-amplitude, only the Fourier coefficients of the shear stress for the first harmonic, $\eta'_{1n}(\omega)$, contribute to the cycle-averaged temperature rise [98].

Although much has been done in developing the molecular theory for the stress tensor, there has been very little done for doing the same for the heat-flux vector. Curtiss and Bird [99] made an initial attempt at doing this, but with limited success. As a result most heat

transfer calculations have been made by using Fourier's law of heat conduction, which does not take into account the alignment of the polymer molecules in flow and the attendant anisotropic effects.

X. CONCLUSION

With regard to the *continuum models* we feel that the corotational models are to be preferred over the convected models. The former are somewhat simpler mathematically than the latter, there being no need to get involved with the notation of general tensor analysis, with its covariant and contravariant components and derivatives. Even the elementary Maxwell-type expressions show a preference for the corotational form, which gives results for a wide variety of rheological functions that are more nearly in line with the experimental data than the corresponding convected form.

Similarly, with regard to the *molecular models*, the Hookean dumbbell is less satisfactory as an elementary model than the rigid dumbbell. However, by introducing finitely extensible nonlinear springs (as in the FENE and FENE-P models), generally good results can be obtained. It is remarkable that the rigid dumbbell gives qualitatively correct results for many rheological functions, for both

solutions and polymer melts, indicating that it is the orientation of the constituent molecules that is more important than the detailed motion of the individual parts of the polymer chains.

In this review, we have discussed only *differential* constitutive equations. A similar review of *integral* constitutive equations could also be given. Here, by far the largest number of publications have appeared for the convected integral models, possibly because of the influence of Lodge [47], whose book showed the connection between network theory for a polymer melt and a single integral constitutive equation, called the "rubberlike liquid." On the other hand the corotational integral formalism, pioneered by Goddard and Miller [100], although not based on a molecular theory, produces a "memory integral expansion" that has better convergence properties than its codeformational counterpart [43]. The corotational integral models have never gained the popularity that the convected models have enjoyed, possibly because of the perceived difficulty in evaluating the kinematic tensor appearing in the integrals.

We have also focused on the single-molecule theories, ignoring the "tube models" that have been explored in the past three decades [101,102]. By *tube models*, we mean, molecular models that constrain chains to move along their axes by imagining them inside tubes.

Although the tube models may successfully describe equilibrium properties and diffusion, without drastic empirical modifications of the original "tube" idea, they enjoy less success in describing rheological phenomena. For instance, the tube model fails to predict either rod-climbing [103] or recoil [104].

In this review, we focus on the elementary dumbbell models, ignoring much of the work that has been done on chain models, branched chain models, ring models, and others (see Table 16.4-1 of [8]). Moving beyond the dumbbell models involves much more difficult mathematics and we feel that time is still well spent on elementary models. We have seen that these have a great deal to teach us regarding methodology and that they help us get at the key physical ideas.

XI. ACKNOWLEDGMENT

This research was undertaken, in part, thanks to support from the Vilas Trust Fund at the University of Wisconsin-Madison for the Vilas Professorship. This research was also undertaken, in part, thanks to funding from the Canada Research Chairs program of the Government of Canada for the Natural Sciences and Engineering

Research Council of Canada (NSERC) Tier 1 Canada Research Chair in Rheology.

A.J. Giacomin is indebted to the Faculty of Applied Science and Engineering of Queen's University at Kingston, for its support through a Research Initiation Grant (RIG). We further acknowledge Mr. Chaimongkol Saengow of the Mechanical and Aerospace Engineering Department of King Mongkut's University of Technology North Bangkok (Thailand) for his generous help with Section IV. We thank Dr. Andrew M. Schmalzer of the Los Alamos National Laboratory for contributing Figure **1** and Figure **2**.

Table I: Equivalence of Molecular and Continuum Parameters

Constants	Rigid Dumbbell (a)	FENE Dumbbell (b)
η_p	$nkT\lambda$	$\frac{bnkT\lambda_H}{b+5}$
λ_1	λ	$\frac{b(2b+11)\lambda_H}{(2b+7)(b+9)}$
λ_2	$\frac{2}{5}\lambda$	$\frac{-14b\lambda_H}{(2b+7)(b+7)(b+9)}$
μ_1	$-\frac{1}{7}\lambda$	$\frac{b(2b+3)\lambda_H}{(2b+7)(b+9)}$
μ_2	$-\frac{26}{35}\lambda$	$\frac{-2b(4b+21)\lambda_H}{(2b+7)(b+7)(b+9)}$
μ_0	$-\frac{2}{7}\lambda$	$\frac{-6b\lambda_H}{(2b+7)(b+5)(b+9)}$

(a) See pp. 555 & 571 of [29], and p. 407 of [11].
(b) See pp. 499-500 of [29] and p. 407 of [11]. This is the FENE dumbbell without the Peterlin approximation.

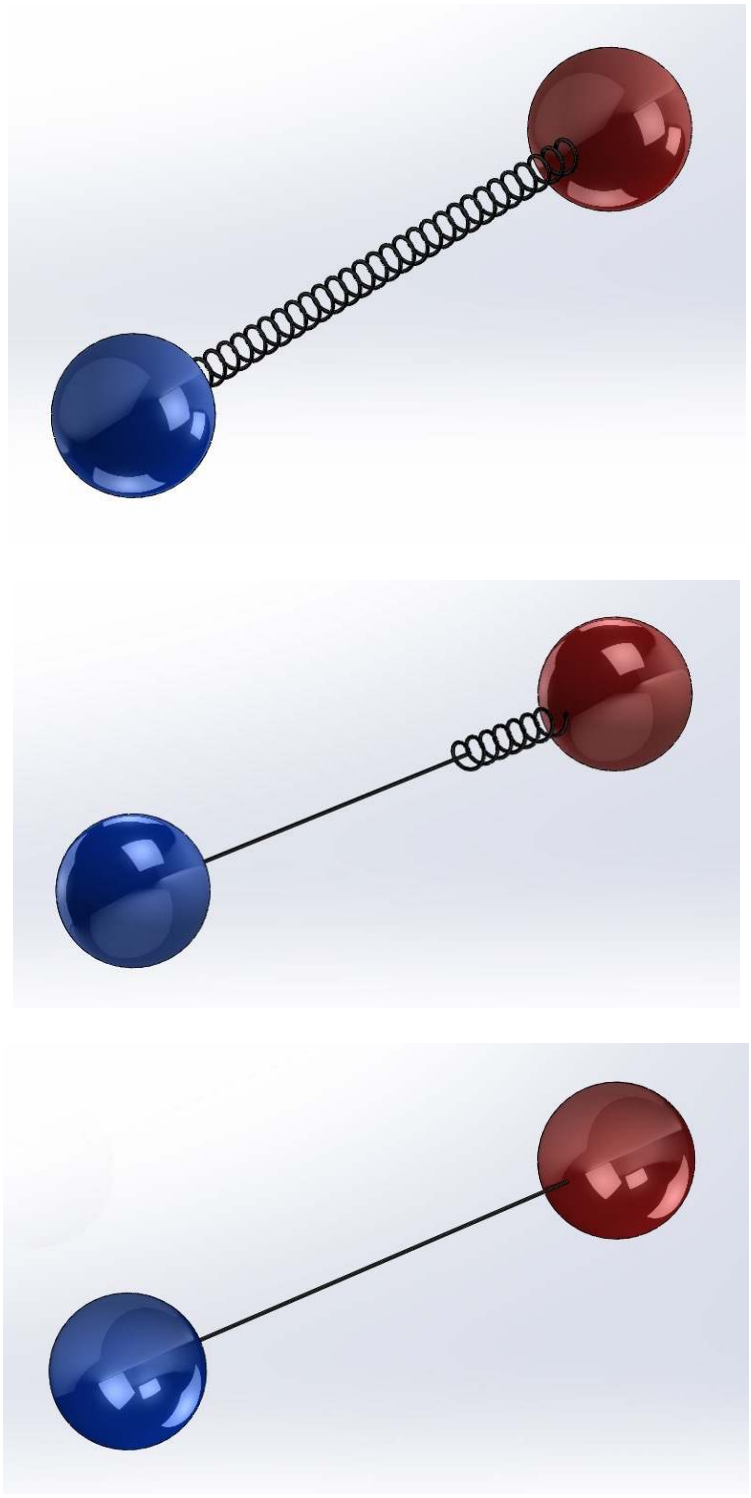

Figure 1: Elastic (top), Fraenkel (middle), and Rigid (bottom) dumbbells.

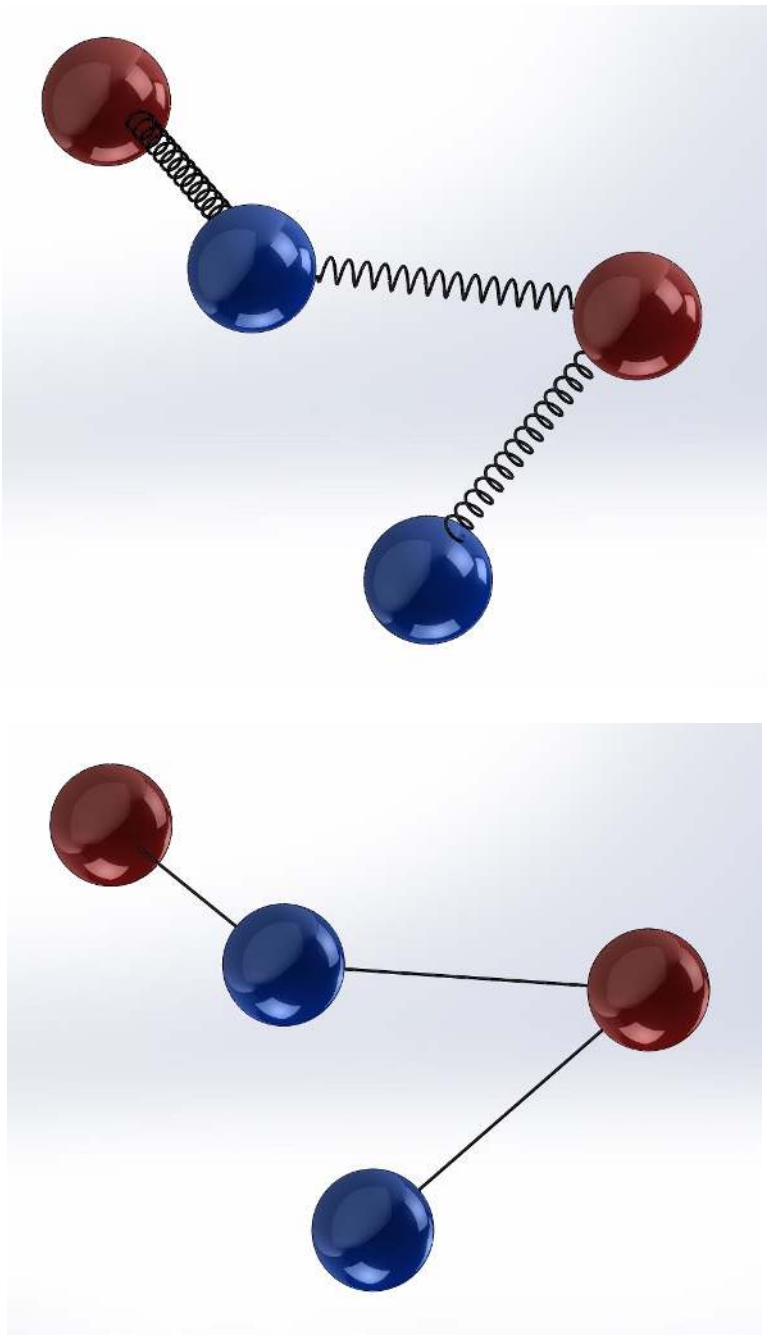

Figure 2: Rouse or Zimm freely-jointed, (top), and Kramers freely-jointed (bottom) chains, $\left(N = 4\right)$.

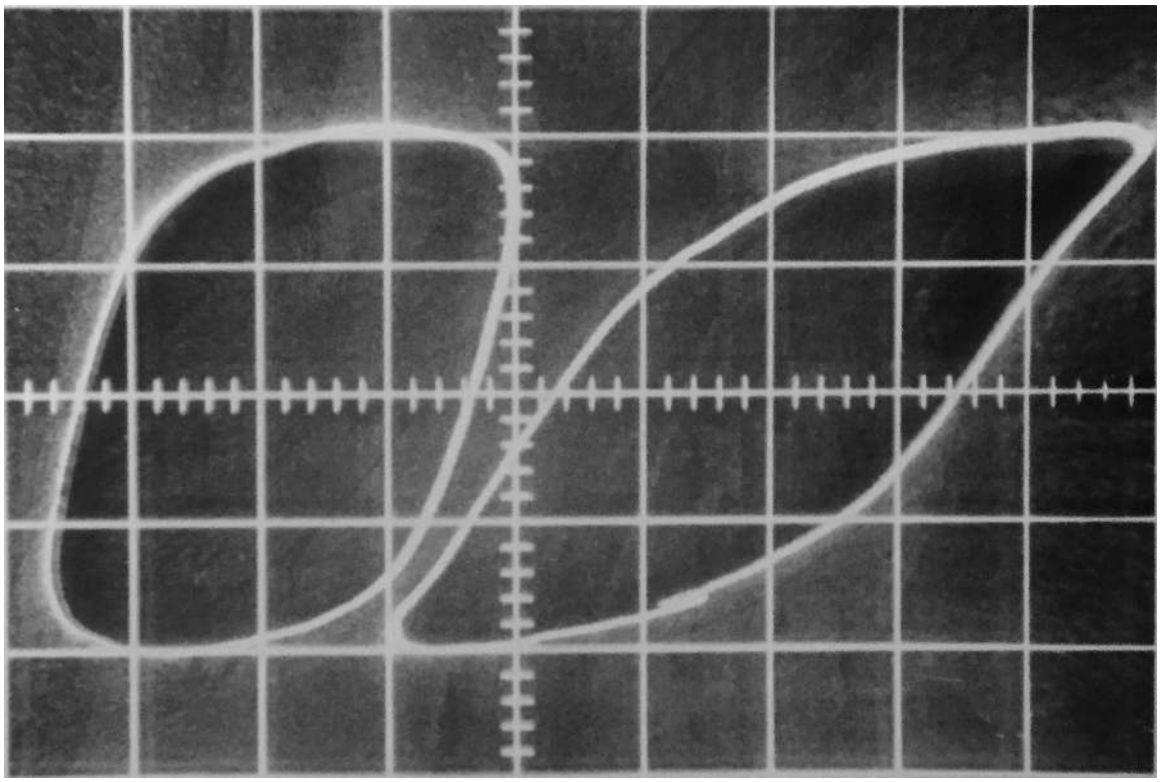

Figure 3: Large-amplitude oscillatory shear loops of $-\tau_{yx}(t)$ *versus* $\int_0^t \dot{\gamma}(t)\,dt = \left[\dot{\gamma}^0/\omega\right]\sin\omega t$ (left) and *versus* $\dot{\gamma}^0\cos\omega t$ (right) for polyisobutylene melt (Vistanex LM-MS [67,68,105]) at room temperature ($\omega = 2\pi/5\,\mathrm{rad/s}$, $\dot{\gamma}^0 = 20.6\,\mathrm{s}^{-1}$, $\tau_{yx,\max} = 0.0793\,\mathrm{MPa}$).

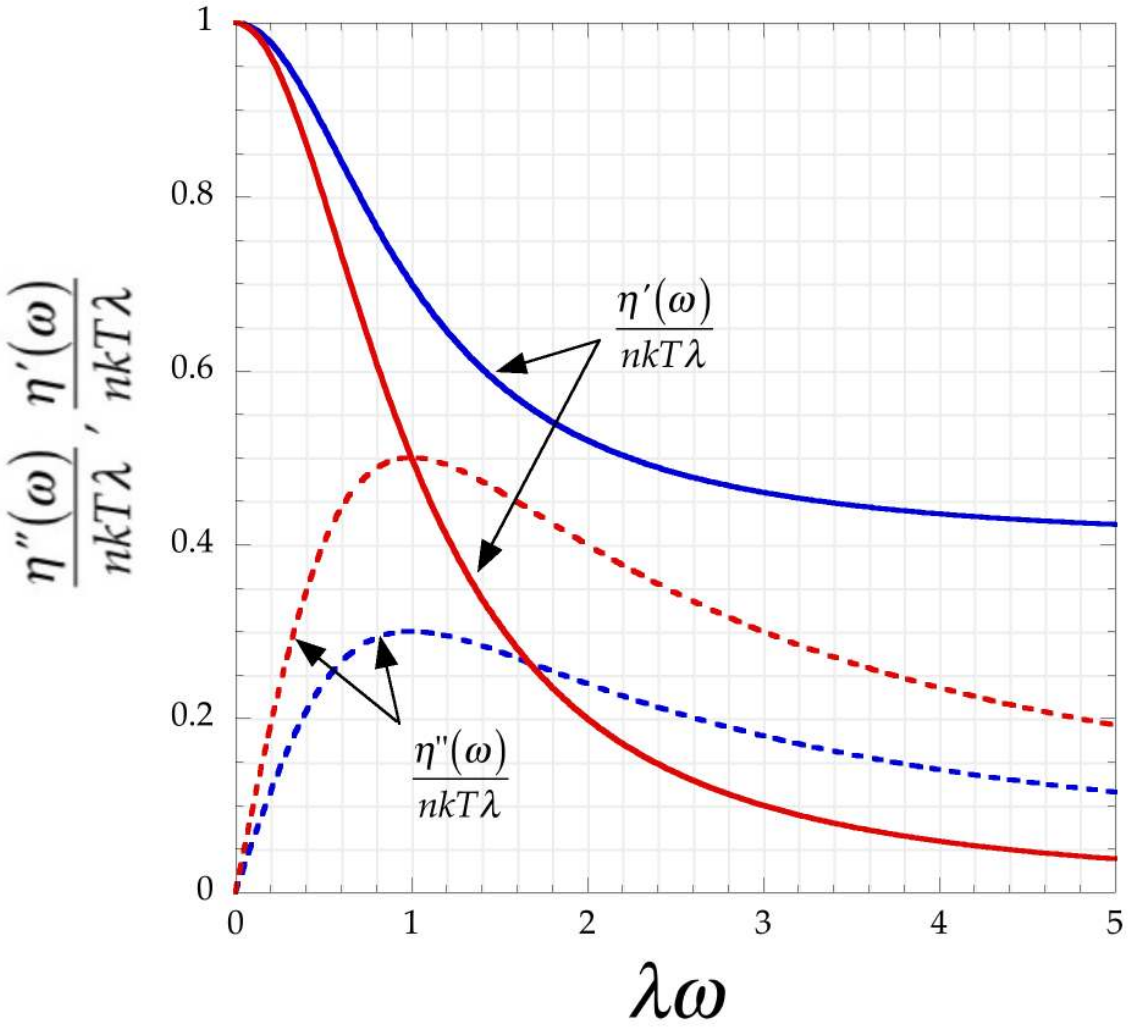

Figure 4: The rigid dumbbell model (blue) versus the corotational Maxwell model (red) for small-amplitude oscillatory shear: $\eta'(\lambda\omega)$ [Eq. (49) versus (41), solid curves] and $\eta''(\lambda\omega,\dot{\gamma}^0)$ [Eq. (50) versus (48), dashed curves].

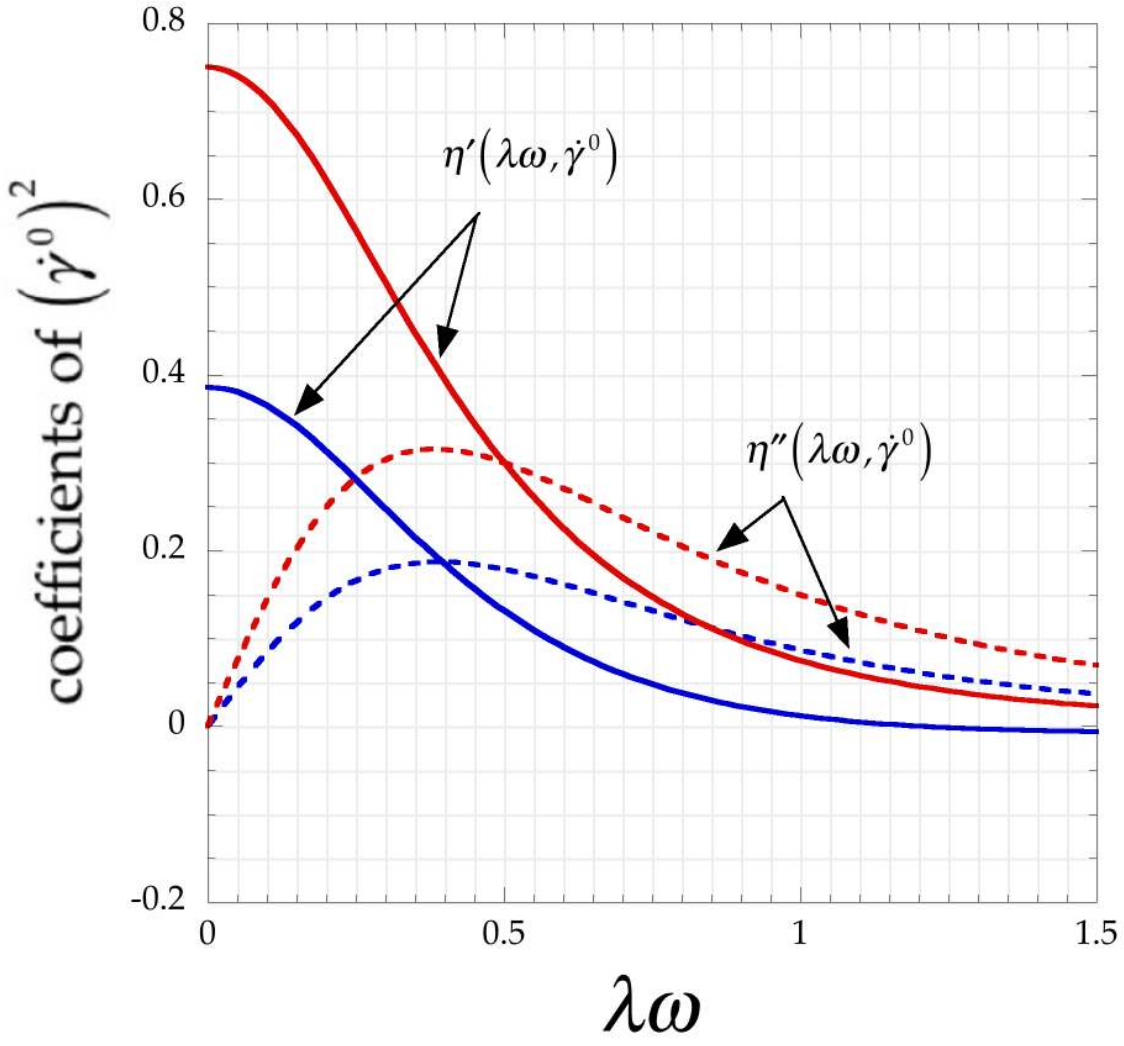

Figure 5: The rigid dumbbell model (blue) versus the corotational Maxwell model (red) for large-amplitude oscillatory shear: Coefficients of $\left(\dot{\gamma}^0\right)^2$ in expressions for $\eta'\left(\lambda\omega,\lambda\dot{\gamma}^0\right)$ [Eq. (88) versus (90) of [88] for $\eta'_{13}\left(\omega\right)$, solid curves] and for $\eta''\left(\lambda\omega,\lambda\dot{\gamma}^0\right)$ [Eq. (89) versus (91) of [88] for $\eta''_{13}\left(\omega\right)$, dashed curves].

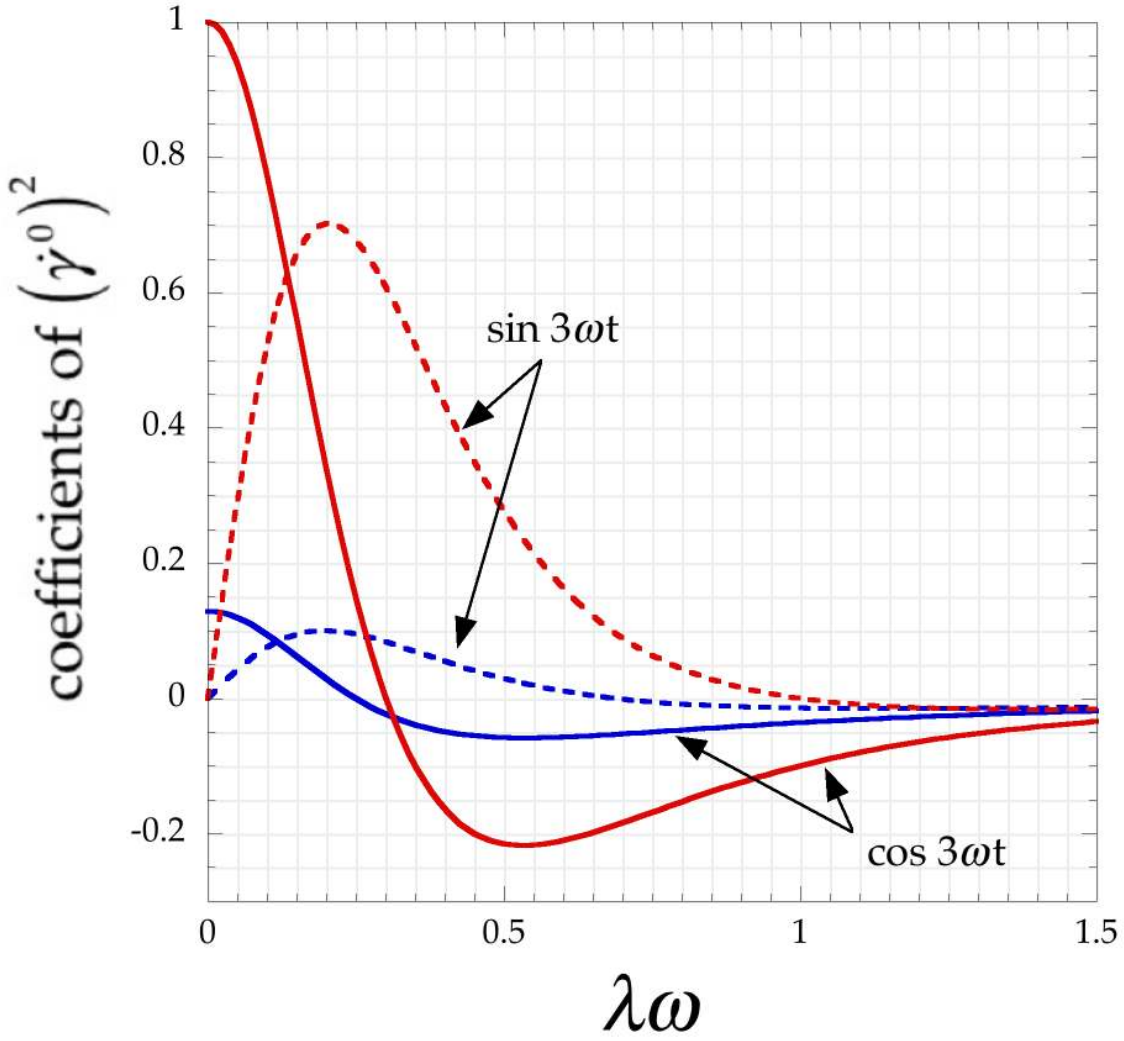

Figure 6: The rigid dumbbell model (blue) versus the corotational Maxwell model (red) for large-amplitude oscillatory shear: Coefficients of $\left(\dot{\gamma}^0\right)^2$ in expressions for the $\cos 3\omega t$ term [Eq. (92) versus (94) of [88] for $\eta'_{33}(\omega)$, solid curves] and for the $\sin 3\omega t$ term [Eq. (93) versus (95) of [88] for $\eta''_{33}(\omega)$, dashed curves].

XII. REFERENCES

[1] Bird RB, Stewart WE, Lightfoot EN, Klingenberg DJ. 2015. *Introductory Transport Phenomena*. New York: Wiley

[2] Maxwell JC. 1867. On the dynamical theory of gases. *Phil. Trans. Roy. Soc. London.* A157:49-88

[3] Bird RB, Curtiss CF, Armstrong RC, Hassager, O. 1987. *Dynamics of Polymeric Liquids*, 2d edition, *Vol. 1, Fluid Dynamics*. New York: Wiley. Erratum: In the first printing, the entry for b_3 in column 3 of Table 6.2-2 "$\eta_0\lambda_1(\lambda_1(\lambda_1-\lambda_2)$" should be "$\eta_0\lambda_1(\lambda_1-\lambda_2)$".

[4] Oldroyd JG. 1950. On the formulation of rheological equations of state. *Proc. Roy. Soc. London.* A200:523-41

[5] Jeffreys H. 1924. *The Earth: Its Origin, History and Physical Constitution*, London: Cambridge University Press

[6] Jeffreys H. 1929. *The Earth: Its Origin, History and Physical Constitution*, 2d edition, London: Cambridge University Press

[7] Spriggs TW. 1965. A four-constant model for viscoelastic fluids. *Chem. Eng. Sci.* 20:931-40

[8] Bird RB, Curtiss CF, Armstrong RC, Hassager O. 1987. *Dynamics of Polymeric Liquids*, 2d edition, *Vol. 2, Kinetic Theory*. New York: Wiley

[9] Zaremba S. 1903. Le principe des mouvements relatifs et les équations de la mécanique physique. *Bull. Int. Acad. Sci. Cracovie.* 594-614

[10] Giacomin AJ, Bird RB. 2011. Normal stress differences in large-amplitude oscillatory shear flow for the corotational "ANSR" model. *Rheologica Acta*. 50(9):741-52. Errata: In Eqs. (47) and (48), "$20\mathrm{De}^2$" and "$10\mathrm{De}^2-50\mathrm{De}^4$" should be "$20\mathrm{De}$" and "$10\mathrm{De}-50\mathrm{De}^3$".

[11] Bird RB, Armstrong RC, Hassager O. 1977. *Dynamics of Polymeric Liquids,* 1st edition, *Vol. 1, Fluid Mechanics*. New York: Wiley

[12] Jaumann G. 1905. *Grundlagen der Bewegungslehre*, Johann Ambrosius Barth, Leipzig

[13] Jaumann G. 1911. *Sitzungsberichte Akad. Wiss. Wien, IIa*, 120:385-530

[14] Fromm H. 1947; 1948. Laminare Strömung Newtonscher und Maxwellscher Flüssigkeiten. *Zeits. für angew. Math. u. Mech.*, 25/27:146-50; 28:43-54

[15] DeWitt TW. 1955. A rheological equation of state which predicts non-Newtonian viscosity, normal stresses, and dynamic moduli," *J. Appl. Phys.*, 26:889-94

[16] Oldroyd JG. 1958. Non-Newtonian effects in steady motion of some idealized elasto-viscous fluids. *Proc. Roy. Soc.* A245:278-97

[17] Giacomin AJ, Bird RB, Johnson LM, Mix AW, 2011. Large-Amplitude Oscillatory Shear Flow from the Corotational Maxwell Model. *Journal of Non-Newtonian Fluid Mechanics*, 166(19-20):1081–1099. Errata: after Eq. (20), Ref. [10] should be [13]; in Eq. (66), "$20\mathrm{De}^2$" and "$10\mathrm{De}^2-50\mathrm{De}^4$" should be "$20\mathrm{De}$" and "$\left(10\mathrm{De}-50\mathrm{De}^3\right)\mathrm{De}$" and so Fig. 15 through Fig. 17 of [90] below replace Figs. 5-7; on the ordinates of Figs. 5-7, $\frac{1}{2}$ should be 2; after Eq. (119), "$(\zeta\alpha)$" should be "$\zeta(\alpha)$"; in Eq. (147), "$n-1$" should be "$n=1$"; in Eqs. (76) and (77), Ψ' and Ψ'' should be Ψ_1' and Ψ_1''; throughout, Ψ_1^d, Ψ_1' and Ψ_1'' should be Ψ_1^d, Ψ_1' and Ψ_1''; in Eq. (127), "$\cos\tau$" should be "$(-\cos\tau)$"; after Eq. (136), "Eq. (134)" should be "Eqs. (133) and (135)" and "Eq. (135)" should be "Eqs. (134) and (135)"; after Eq. (143), $|\tau_{yx}|$ should be $\dot{\gamma}$; in Eqs. (181) and (182), "1,21" should be "1,2"; after Eq. (184) and in Eq. (185), "mp" should be "$1,mp$"; Eq. (65) should be $\mathrm{We}/\mathrm{De} > \sqrt[h_{\mathbb{N}}]{(h_{\mathbb{N}}+1)!}$; after Eq. (65), $\sqrt[3]{3!}$ should be $\sqrt[4]{5!}$, and $\gamma_0 > 1.82$ should be $\gamma_0 > 3.31$; see also [18] below.

[18] Giacomin AJ, Bird RB, Johnson LM, Mix AW. 2012. Corrigenda: "Large-Amplitude Oscillatory Shear Flow from the Corotational Maxwell Model," [Journal of Non-Newtonian Fluid Mechanics **166**,

1081–1099 (2011)]. *Journal of Non-Newtonian Fluid Mechanics*. 187/188:48-48. [See [17] above].

[19] Williams MC, Bird RB, 1962. Three-constant Oldroyd model for viscoelastic fluids," *Physics of Fluids*, 5:1126-1127

[20] Oakley JG, Yosick JA, Giacomin AJ. 1998. Molecular origins of nonlinear viscoelasticity. *Mikrochimica Acta*. 130:1-28

[21] Peterlin, A. 1968. Non-Newtonian viscosity and the macromolecule. *Adv. in Macromolecular Chemistry*. 1**:**225-81

[22] Fan X-J. 1985. Viscosity, first normal-stress coefficient, and molecular stretching in dilute polymer solutions. *J. Non-Newt. Fluid Mech*., 17:125-144

[23] Fraenkel GK. 1952. Visco-elastic effect in solutions of simple particles. *J. Chem. Phys.* 20:1958-64

[24] Bird RB, Curtiss CF, Beers KJ. 1997. Polymer contribution to the thermal conductivity and viscosity in a dilute solution (Fraenkel Dumbbell model). *Rheologica acta*, 36(3):269-76

[25] Fraenkel GK. 1949. The viscosity and shear elasticity of solutions of simple deformable particles, PhD Thesis, Cornell University, Ithaca

[26] Giesekus H. 1956. Das Reibungsgesetz der strukturviskose Flüssigkeit. *Kolloïd-Z.* 147:29-41. Erratum: 1961 Einige Bemerkungen zm Fliessverhalten elastoviskoser Flüssigkeiten.

[27] Bird RB, Warner HR Jr, Evans DC. 1972. Kinetic theory and rheology of dumbbell suspensions with Brownian motion. *Adv. Polym. Sci.* 8:1-90

[28] Bird RB, Armstrong RC. 1972. Time-dependent flows of dilute solutions of rodlike macromolecules. *J. Chem. Phys.* 56:3680-82

[29] Bird RB, Hassager O, Armstrong RC, Curtiss, C. 1977. *Dynamics of Polymeric Liquids, 1st Edition, Vol. 2, Kinetic Theory*. New York: Wiley

[30] Rouse PE. A theory of the linear viscoelastic properties of dilute solutions of coiling polymers. 1953. *J. Chem. Phys.* 21:1272-80

[31] Zimm BH. 1956. Dynamics of polymer molecules in dilute solution: viscoelasticity, flow birefringence and dielectric loss. *J. Chem. Phys.* 24:269-78. Errata: see Williams MC. 1965. *J. Chem. Phys.* 42:2988-89.

[32] Kramers HA. 1944. Het gedrag van macromoleculen in een stroomende vloeistof. *Physica*. 11:1-19

[33] Hassager O. 1974. Kinetic theory and rheology of bead-rod models for macromolecular solutions. I. Equilibrium and steady flow properties. *J. Chem. Phys.* 60:2111-24

[34] Curtiss CF, Bird RB. 1981. A kinetic theory for polymer melts. I. The equation for the single-link orientational distribution function. *J. Chem. Phys.* 74:2016-25

[35] Curtiss CF, Bird RB. 1981. A kinetic theory for polymer melts. II. The stress tensor and the rheological equation of state. *J. Chem. Phys.* 74:2026-33

[36] Bird RB, Saab HH, Curtiss CF. 1982. A kinetic theory for polymer melts. 3. Elongational flows. *The Journal of Physical Chemistry*. 86(7):1102-06

[37] Bird RB, Saab HH, Curtiss CF. 1982. A kinetic theory for polymer melts. IV. Rheological properties for shear flows. *The Journal of Chemical Physics*. 77(9):4747-57

[38] Saab HH, Bird RB, Curtiss CF. 1982. A kinetic theory for polymer melts. V. Experimental comparisons for shear-flow rheological properties. *The Journal of Chemical Physics*, *77*(9):4758-66

[39] Schieber JD, Curtiss CF, Bird RB. 1986. Kinetic theory of polymer melts. 7. Polydispersity effects. *Industrial & Engineering Chemistry Fundamentals*. 25(4):471-75

[40] Schieber JD. 1987. Kinetic theory of polymer melts. VIII. Rheological properties of polydisperse mixtures. *The Journal of Chemical Physics*, *87*(8):4917-27.

[41] Schieber JD. 1987. Kinetic theory of polymer melts. IX. Comparisons with experimental data. *The Journal of Chemical Physics*. 87(8), 4928-36.

[42] Abdel-Khalik SI, Hassager O, Bird RB. 1974. The Goddard expansion and the kinetic theory for solutions of rodlike macromolecules. *J. Chem. Phys.* 61:4312-16

[43] Bird RB, Hassager O, Abdel-Khalik SI. 1974. Co-rotational rheological models and the Goddard expansion. *AIChE J.* 20:1041-66

[44] Bird RB. 1972. A modification of the Oldroyd model for rigid dumbbell suspensions with brownian motion. *J. Appl. Math. Phys.* (*ZAMP*). 23:157-59

[45] Winter HH, Baumgärtel M, Soskey PR. 1993. A parsimonious model for viscoelastic fluids and solids. *Techniques in Rheological Measurement*. Collyer (ed.). London and New York: Chapman and Hall; Dordrecht (The Netherlands) Kluwer Academic Publishers; pp. 123-60 (Chapter 5)

[46] Goddard JD, Miller C. 1966. An inverse for the Jaumann derivative and some applications to the rheology of viscoelastic fluids. *Rheol. Acta*. 5:177-84

[47] Lodge AS. 1964. *Elastic Liquids*. New York: Academic Press. Errata: Eq. (6.40a) should be $s = \alpha\left\{\sin\omega t\left(1-\cos\omega\tau\right)+\cos\omega t\sin\omega\tau\right\}$; Eq. (6.40b) should be $s^2 = \alpha^2\left\{1+\cos 2\omega\tau\cos\omega\tau+\sin 2\omega t\sin\omega\tau\right\}\left(1-\cos\omega\tau\right)$; Eq. (6.41a) should be $p_{11}-p_{22} = \alpha^2\left\{A+B\cos 2\omega t+C\sin 2\omega t\right\}$; Eq. (6.41b) should be $p_{21} = \alpha\left\{D\cos\omega t+A\sin\omega t\right\}$; in line 4 of p. 113, $\alpha A\cos\omega t$ should be $\alpha D\cos\omega t$; in the sentence preceding Eq. (6.43), and also in Eq. (6.43), "the out-of-phase part of p_{21}" should be "the part of p_{21} that is in-phase with s".

[48] Kim S, Fan XJ. 1984. A perturbation solution for rigid dumbbell suspensions in steady shear flow. *J. Rheol.* 28:117-22

[49] Stewart WE, Sørensen JP. 1984. Hydrodynamic interaction effects in rigid dumbbell suspensions. II. Computations for steady shear flow. *Trans. Soc. Rheol.* 16:1-13

[50] Öttinger HC. 1988. A note on rigid dumbbell solutions at high shear rates. *J. Rheol.* 32:135-143. Errata: (1988) *J. Rheol.* 32:814

[51] Cox WP, Merz EH. 1958. Correlation of dynamic and steady flow viscosities. *J. Polymer Sci.* 28:619-22

[52] Laun HM. 1986. Prediction of elastic strains of polymer melts in shear and elongation. *J Rheol.* 30:459-501

[53] Ferry JF. 1980. *Viscoelastic Properties of Polymers*. 3rd ed. New York: Wiley

[54] Giacomin AJ, Dealy JM. 1993. Large-amplitude oscillatory shear. Chapter 4, Collyer AA, ed. *Techniques in Rheological Measurement*, Chapman and Hall, London & New York, pp. 99-121; Kluwer Academic Publishers, Dordrecht, pp. 99-121

[55] Giacomin AJ, Dealy JM. 1998. Using large-amplitude oscillatory shear. Chapter 11, Collyer AA, Clegg DW, eds. *Rheological Measurement*, 2nd ed., Kluwer Academic Publishers, Dordrecht, Netherlands, pp. 327-56

[56] Hyun K, Wilhelm M, Klein CO, Cho KS, Nam JG, Ahn KH, Lee SJ, Ewoldt RH, McKinley GH. 2011. A review of nonlinear oscillatory shear tests: analysis and application of large amplitude oscillatory shear (LAOS). *Prog. Polym. Sci.* 36:1697–753

[57] Giacomin AJ, Oakley JG. 1993. Obtaining Fourier series graphically from large amplitude oscillatory shear loops. *Rheologica Acta*. 32:328-32

[58] Fan X-J, Bird RB. 1984. A kinetic theory for polymer melts VI. calculation of additional material functions. *J. Non-Newt. Fluid Mech*. 15:341-73

[59] Ewoldt RH, Hosoi AE, McKinley GH, 2008. New measures for characterizing nonlinear viscoelasticity in large amplitude oscillatory shear. *J. Rheol*. 52:1427-58

[60] Ewoldt RH, 2009. Nonlinear viscoelastic materials: bioinspired applications and new characterization measures. Ph.D. Thesis, Mechanical Engineering Department, Massachusetts Institute of Technology, Cambridge, MA.

[61] Ewoldt RH, McKinley GH. 2010. "On secondary loops in LAOS via self-intersection of Lissajous–Bowditch curves," *Rheol. Acta*. 49:213-19

[62] Jeyaseelan RS, Giacomin AJ, 1994. How affine is the entanglement network of molten low-density polyethylene in large amplitude oscillatory shear? *Journal of Engineering Materials and Technology*. 116(1):14-18

[63] Gordon RJ, Schowalter WR. 1972. Anisotropic fluid theory: a different approach to the dumbbell theory of dilute polymer solutions. *Transactions of The Society of Rheology*. 16(1):79-97

[64] Dealy JM, Petersen JF, Tee T-T. 1973. A concentric-cylinder rheometer for polymer melts. *Rheol. Acta*. 12:550-58

[65] Tee T-T, Dealy JM. 1975. Nonlinear viscoelasticity of polymer melts. *Trans. Soc. Rheol*. 19:595-615

[66] Tee T-T. 1974. Large amplitude oscillatory shearing of polymer melts. PhD Thesis, Chemical Engineering Dept., McGill University, Montréal, Canada

[67] Soong SS. 1983. A parallel plate viscoelastometer for molten polymers. PhD Thesis, Chemical Engineering Dept., McGill University, Montréal, Canada

[68] Dealy JM, Soong SS. 1984. A parallel plate melt rheometer incorporating a shear stress transducer. *Journal of Rheology*. 28(4):355-65

[69] Wilhelm M, Maring D, Spiess H-W, 1998. Fourier-transform rheology. *Rheologica Acta*. 37(4):399-405

[70] Wilhelm, M., 2000. Fourier-transform rheology. Thesis for the German *Habilitation*, Max-Planck-Institut für Polymerforschung, Mainz, Germany.

[71] Wilhelm M. 2002. Fourier-transform rheology. *Macromolecular Materials and Engineering*. 287(2):83-105

[72] Ahirwal D, Filipe S, Schlatter G, Wilhelm M, 2014. Large amplitude oscillatory shear and uniaxial extensional rheology of blends from

linear and long-chain branched polyethylene and polypropylene. *Journal of Rheology*. 58(3):635-58

[73] Hyun K, Wilhelm M. 2009. Establishing a new mechanical nonlinear coefficient Q from FT-rheology: first investigation of entangled linear and comb polymer model systems. *Macromolecules*. 42:411-22

[74] Onogi S, Masuda T, Matsumoto T. 1970. Non-Linear Behavior of Viscoelastic Materials. I. Disperse Systems of Polystyrene Solution and Carbon Black. *Transactions of The Society of Rheology*. 14(2):275-94

[75] Matsumoto T, Segawa Y, Warashina Y, Onogi S. 1973. Nonlinear behavior of viscoelastic materials. II. The method of analysis and temperature dependence of nonlinear viscoelastic functions. *Transactions of The Society of Rheology*. 17(1):47-62

[76] Davis WM, Macosko CW. 1978. Nonlinear dynamic mechanical moduli for polycarbonate and PMMA. *Journal of Rheology*. 22(l):53-71

[77] Pearson DS, Rochefort WE. 1982. Behavior of concentrated polystyrene solutions in large-amplitude oscillating shear fields. *J. Polym. Sci.: Pol. Phys. Ed.* 20, 83; Errata: on p. 95, $e^{i\omega s}$ should be $e^{-i\omega s}$ in Eq. (A2); after Eq. (A10), α should be $\sqrt{\omega\tau_d/2}$; and in Eq. (A11), $\cos x$ should be $\cosh x$; in Eq. (A7), $\sqrt{2\alpha}$ should be $\sqrt{2}\alpha$.

[78] Helfand E, Pearson DS. 1982. Calculation of the nonlinear stress of polymers in oscillatory shear fields. *J. Polym. Sci.: Pol. Phys. Ed*. 20:1249-58. Erratum: In Eq. (17), "Im" should be "Re".

[79] Reinheimer K, Wilhelm M, 2013. April-Science: Charakterisierung von Hellen und Dunklen Bierschäumen durch Mechanische Obertonanalyse, FT-Rheologie, Bunsen-Magazin," *Zeitschrift für physikalische Chemie*. 15(1):52-55

[80] Dötsch T, Pollard M, Wilhelm M. 2003. Kinetics of isothermal crystallization in isotactic polypropylene monitored with rheology and Fourier-transform rheology. *Journal of Physics: Condensed Matter*. 15:S923–S931

[81] Dingenouts N, Wilhelm M. 2010. New developments for the mechanical characterization of materials," *Korea-Australia Rheology Journal*. 22(4):317-30

[82] Giacomin AJ, Gilbert PH, Merger D, Wilhelm M. 2015. Large-amplitude oscillatory shear: comparing parallel-disk with cone-plate flow. *Rheologica Acta*. 54:263-85

[83] Oakley JG. 1992. Measurement of normal thrust and evaluation of upper-convected Maxwell models in large amplitude oscillatory shear. Masters Thesis, Texas A&M University, Mechanical Engineering Dept., College Station, TX

[84] Oakley JG, Giacomin AJ. 1994. A sliding plate normal thrust rheometer for molten plastics. *Polymer Engineering and Science*. 34(7): 580-84

[85] Lodge AS. 1961. Recent network theories of the rheological properties of moderately concentrated polymer solutions," in *Phénomènes de Relaxation et de Fluage en Rhéologie Non-linéaire*, Editions du C.N.R.S., Paris, pp. 51-63

[86] Saengow C, Giacomin AJ, Kolitawong C. 2015. Exact analytical solution for large-amplitude oscillatory shear flow. *Macromolecular Theory and Simulations*. 23, DOI: 10.1002/mats.201400104, pp. 1-41

[87] Giacomin AJ, Saengow C (ชยั มงคล แซ่โง้ว), Guay M, Kolitawong C (ชาญยุทธ โกลิตะวงษ์). 2015. Padé approximants for large-amplitude oscillatory shear flow. *Rheologica Acta*. 54:679693

[88] Bird RB, Giacomin AJ, Schmalzer AM, Aumnate C. 2014. Dilute rigid dumbbell suspensions in large-amplitude oscillatory shear flow: shear stress response. *The Journal of Chemical Physics*. 140:074904; Corrigenda: In Eq. (91), η' should be η''; In caption to Fig. 3, "$\psi_1\left[P_2^2 s_2\right]$" should be "$\cos 3\omega t$" and "$\psi_2\left[P_2^0 c_0, P_2^2 c_2, \ldots\right]$" should be "$\sin 3\omega t$"; in Eq. (6), "38725" should be "38728".

[89] Schmalzer AM, Bird RB, Giacomin AJ. 2014. Normal stress differences in large-amplitude oscillatory shear flow for dilute rigid dumbbell suspensions," PRG Report No. 002, QU-CHEE-PRG-TR--

2014-2, Polymers Research Group, Chemical Engineering Dept., Queen's University, Kingston, CANADA.

[90] Schmalzer AM, Bird RB, Giacomin AJ. 2015. Normal stress differences in large-amplitude oscillatory shear flow for dilute rigid dumbbell suspensions. *Journal of Non-Newtonian Fluid Mechanics*. 222:56-71. Errata: Above Eqs. (14) and (25), "significant figures" should be "16 significant figures"; in Eq. (10), "38725" should be "38728".

[91] Schmalzer AM, Giacomin AJ. 2015. Orientation in large-amplitude oscillatory shear. Cover Article, *Macromolecular Theory and Simulations*, 24(3):171,181-207. Errata: From 6th line of **Introduction**, delete "small-amplitude oscillatory shear"; in Ref. [22], "[23]" should be "[21]".

[92] Bird RB, Armstrong RC. 1972. Time-dependent flows of dilute solutions of rodlike macromolecules. *J. Chem. Phys.* 56:3680-82. Addendum: In Eq. (8), the term $-\frac{1}{432}\left[\frac{3}{49}\left(\frac{7}{3},0,1\right);t+\frac{3}{537}\left(0,\frac{7}{3},1;t\right)\right]P_4^2 s_2$ should be inserted just before the "+ additional terms".

[93] Park OO, Fuller GG. 1985. Dynamics of rigid dumbbells in confined geometries: Part II. Time-dependent shear flow. *J. Non-Newton. Fluid. Mech.* 18:111-22.

[94] Park OO. 1985. Dynamics of rigid and flexible polymer chains: part 1. transport through confined geometries, PhD Thesis, Chemical Engineering, Stanford University, Stanford, CA

[95] Bird RB, Giacomin AJ, Schmalzer AM, Aumnate C. 2014. Dilute rigid dumbbell suspensions in large amplitude shear flow: Shear stress response. *J. Chem. Phys.* 140:074904

[96] Giacomin AJ, Bird RB, Aumnate C, Mertz AM, Schmalzer AM, Mix AW. 2012. Viscous heating in large amplitude oscillatory shear flow. *Physics of Fluids*. 24:103101

[97] Ding F, Giacomin AJ, Bird RB, Kweon C-B. 1999. Viscous dissipation with fluid inertia in oscillatory shear flow. *Journal of Non-Newtonian Fluid Mechanics*. 86(3):359-374

[98] Giacomin AJ, Bird RB, Baek HM (백형민). 2013. Temperature rise in large-amplitude oscillatory shear flow from shear stress measurements. *Industrial & Engineering Chemistry Research*. 52:2008-2017

[99] Curtiss CF, Bird RB. 1996. Statistical mechanics of transport phenomena: Polymeric liquid mixtures. *Advances in Polymer Science*. 25:1-101

[100] Goddard JD, Miller C. 1966. An inverse for the Jaumann derivative and some applications to the rheology of viscoelastic fluids. *Rheol. Acta*. 5:177-84

[101] De Gennes PG. (1979). *Scaling Concepts in Polymer Physics*. Ithaca, NY: Cornell University Press

[102] Doi M, Edwards SF. 1988. *The Theory of Polymer Dynamics* (Vol. 73). Oxford: Oxford University Press

[103] Lodge AS, Schieber JD, Bird RB. 1988. The Weissenberg effect at finite rod-rotation speeds. *The Journal of Chemical Physics*. 88(6):4001-07

[104] Bird RB, Evans DC, Warner Jr HR, 1971. Recoil in macromolecular solutions according to rigid dumbbell kinetic theory. *Applied Scientific Research*. 23(1):185-92

[105] Giacomin AJ, Jeyaseelan RS. 1995. A constitutive theory for polyolefins in large amplitude oscillatory shear. *Polymer Engineering and Science*. 35(9):768-77